AD NUMBER

ADB285530

NEW LIMITATION CHANGE

TO

Approved for public release, distribution unlimited

FROM

Distribution authorized to U.S. Gov't. agencies only; Proprietary Info.; Jun 2002. Other requests shall be referred to US Army Medical Research and Materiel Comd., 504 Scott St., Fort Detrick, MD 21702-5012.

AUTHORITY

USAMRMC ltr, dtd 15 May 2003

AD_____

Award Number: DAMD17-98-1-8122

TITLE: Centrosome Hypertrophy Induced by p53 Mutations Leads to Tumor Aneuploidy

PRINCIPAL INVESTIGATOR: Wilma L. Lingle, Ph.D.

CONTRACTING ORGANIZATION: Mayo Foundation
Rochester, Minnesota 55905

REPORT DATE: June 2002

TYPE OF REPORT: Annual Summary

PREPARED FOR: U.S. Army Medical Research and Materiel Command
Fort Detrick, Maryland 21702-5012

REPORT DOCUMENTATION PAGE

Form Approved
OMB No. 074-0188

1. AGENCY USE ONLY (Leave blank)	2. REPORT DATE	3. REPORT TYPE AND DATES COVERED
	June 2002	Annual Summary (1 Jun 01 - 31 May 02)

4. TITLE AND SUBTITLE
Centrosome Hypertrophy Induced by p53 Mutations Leads to Tumor Aneuploidy

5. FUNDING NUMBERS
DAMD17-98-1-8122

6. AUTHOR(S)
Wilma L. Lingle, Ph.D.

7. PERFORMING ORGANIZATION NAME(S) AND ADDRESS(ES)
Mayo Foundation
Rochester, Minnesota 55905

E-Mail: lingle@mayo.edu

8. PERFORMING ORGANIZATION REPORT NUMBER

9. SPONSORING / MONITORING AGENCY NAME(S) AND ADDRESS(ES)
U.S. Army Medical Research and Materiel Command
Fort Detrick, Maryland 21702-5012

10. SPONSORING / MONITORING AGENCY REPORT NUMBER

11. SUPPLEMENTARY NOTES

12a. DISTRIBUTION / AVAILABILITY STATEMENT
Distribution authorized to U.S. Government agencies only (proprietary information, Jun 02). Other requests for this document shall be referred to U.S. Army Medical Research and Materiel Command, 504 Scott Street, Fort Detrick, Maryland 21702-5012.

12b. DISTRIBUTION CODE

13. ABSTRACT *(Maximum 200 Words)*

This research is designed to test the hypothesis that aneuploidy in some breast tumors is caused by centrosome abnormalities which are induced by alteration in p53 function. Specific mutations in p53 that are associated with breast cancer, aneuploidy, chromosomal instability, and centrosome abnormalities have been identified during the course of this project. We have shown that p53 mutations correlate with an increase in microtubule nucleating capacity; however, no such correlation is indicated with either centrosome size or centrosome number. To test whether or not specific p53 mutations affect different aspects of centrosome function, thus leading to chromosomal instability and/or changes in microtubule nucleation, we have constructed 5 different adenoviral vectors for our mutant p53 studies. Initial experiments with 2 of these mutant p53 vectors indicates that specific p53 mutations do have different effects on centrosome function in cultured cells derived from normal human mammary epithelia. Further experiments are in progress or in the design stage.

14. SUBJECT TERMS
Breast cancer - Aneuploidy, chromosomal instability, p53, centrosomes, centrosome amplification, microtubules

15. NUMBER OF PAGES
51

16. PRICE CODE

17. SECURITY CLASSIFICATION OF REPORT	18. SECURITY CLASSIFICATION OF THIS PAGE	19. SECURITY CLASSIFICATION OF ABSTRACT	20. LIMITATION OF ABSTRACT
Unclassified	Unclassified	Unclassified	Unlimited

Table of Contents

Cover .....

SF 298 2

Introduction 5

Body 5

Key Research Accomplishments 7

Reportable Outcomes 7

Conclusions 9

References ..... NA

Appendices 10

1. *Amplified Centrosomes In Breast Cancer: A Potential Indicator Of tumor Aggressiveness*
2. *Altered Centrosome Structure Is Associated with Abnormal Mitoses in Human Breast Tumors*
3. *Centrosome amplification drives chromosomal instability in breast tumor development*

INTRODUCTION

This research is designed to test the hypothesis that aneuploidy in some breast tumors is caused by centrosome abnormalities which are induced by alteration in p53 function. Specific mutations in p53 that are associated with breast cancer, aneuploidy, chromosomal instability, and centrosome abnormalities have been identified during the course of this project. We have shown that p53 mutations correlate with an increase in microtubule nucleating capacity; however, no such correlation is indicated with either centrosome size or centrosome number. To test whether or not specific p53 mutations affect different aspects of centrosome function, thus leading to chromosomal instability and/or changes in microtubule nucleation, we have constructed 5 different adenoviral vectors for our mutant p53 studies. Initial experiments with 2 of these mutant p53 vectors indicates that specific p53 mutations do have different effects on centrosome function in cultured cells derived from normal human mammary epithelia. Further experiments are in progress or in the design stage.

BODY

As indicated in 1999 Progress Report, I revised my statement of work in order to use a new Mayo Facility for the p53 mutation screening portion of the project. Research Accomplishments to date reflect the Tasks as outlined in the revised Statement of Work.

Task 1 - Quantification of structural and functional centrosome alterations (months 1-12). As reported in the 2000 Progress Report, this Task is complete. Some of the results from this task were published in American Journal of Pathology (155:1941-1951), a reprint of which is presented in Appendix I.

Task 2 – Screen tissues for aneuploidy (months 10-18). This Task and analysis of the data generated is complete. As reported in the 2000 Progress Report, approximately 35 benign and tumor tissues have been analyzed for ploidy using FISH analysis of chromosomes 3, 7, and 17. These data reveal that: 1) all benign tissues were diploid and had normal centrosomes; 2) three of 21 tumors were diploid or near diploid and had essentially normal centrosome size and function; and 3) 18 of 21 tumors were aneuploid and had significant levels of centrosome amplification. **Therefore, we can conclude that tumor aneuploidy correlates with centrosome amplification.** During the past year a manuscript which includes a portion of these results has been accepted for publication in Breast Cancer Research and Treatment (Appendix II). **Further analysis of the data revealed that, regardless of p53 status, centrosome number and centrosome size each have a statistically significant linear correlation with chromosomal instability. However, centrosome function, as measured by microtubule nucleation capacity, does not correlate with chromosomal instability. Interestingly, microtubule nucleation capacity correlates with loss of differentiation as measured by Nottingham grade.** These results were published in PNAS in February 2002 (Appendix III).

Task 3 – Trial site-directed mutagenesis and trial transfection. This Task is complete. A p53 mutated from glycine to serine at amino acid 245 was selected based on its occurrence in Li-Fraumeni families having a high incidence of breast cancers. Normal human mammary epithelial cells (hMEC) and telomerase-immortalized hMEC cells (hTERT-hMEC, obtained from Geron, Inc. under a Materials Transfer Agreement) transfected with the p53 mutant develop a phenotype consistent with the hypothesis; namely centrosome and mitotic spindle abnormalities are present at a much higher frequency in the presence of mutant p53 than they are in normal cells. Due to the difficulties in

achieving consistently high transfection efficiencies using plasmid based-vectors, we have generated adenoviral vectors for Task 6.

Task 4 – p53 mutation/immunohistochemistry status (months 16-30). This Task is complete, and results have been reported in our February 2002 PNAS publication (Appendix III). Normal tissues had no significant p53 immunostaining. Benign tumors had an average value of 3.6% of the cells with p53 immunostaining (ranging from 0 to 10% of the tumor cells). Malignant tumors ranged from 0% (13 of 40 analyzed) to more than 75% (8 of 40 analyzed), with a mean of 13.8%. In summary, we found that 25 tumors had wild type p53 by DHPLC. The 8 tumors indicated by DHPLC as containing possible p53 mutations have been sequenced and the precise mutation has been identified in 8 of the tumors. One of the eight mutations (in exon 6) was silent. The other 7 mutations resulted in changes in the amino acid sequence of p53 in the DNA binding domain. Exons 5, 7, and 8 each had 2 tumors containing mutations, while 1 tumor had a mutation in exon 6. One of the mutations is the commonly occurring R249G mutation; no mutations have been found in exons 4 or 9.

Task 5 – Analysis of data from Tasks 1,2, and 4 (months 31-33). This Task is complete, and the analysis has been published (Appendix III). Centrosome microtubule nucleating capacity in p53 mutant tumors is 2 fold higher than in p53 wild type tumors; this difference is statistically significant. On average, aneuploid tumors with mutant p53 did not have centrosomes that differed significantly in either size or number from those aneuploid tumors with wild type p53. We identified three different p53 mutations (described in Task 6) that appear to have significant effects on centrosome structure and function. The first of these mutants is a termination mutant at amino acid 195. The tumor with this mutation has a high level of chromosomal instability and numerous, large centrosomes per cell. However, it has only a moderate increase in microtubule nucleation capacity. The second mutation is R249G, a commonly mutated codon in many cancers. The tumor with this mutation has centrosomes highly amplified by all measures and a significant level of chromosomal instability. The third mutation, C238F, is in a tumor that is nearly normal in centrosome size and number, but has the highest microtubule nucleation capacity of all the tumors we measured. This tumor has a stable, but aneuploid, karyotype.

Task 6 – Site-directed mutagenesis of p53 using mutants identified in Task 5 (months 33- 36). This Task is complete. We have created high efficiency adenoviral vectors for the three p53 mutations identified in Task 5 and for the Li-Fraumeni mutant identified in Task 3. These mutations are: 1) R196stop, in which a mutation of C to T at base 586 in exon 6 codes for STOP instead of Arginine, truncating the protein at 195 amino acids; 2) C238F, in which a G to T mutation at base 713 in exon 7 codes for phenylalanine instead of cysteine at codon 238; 3) R249G, in which mutation of A to G at base 745 in exon 7 codes for glycine instead of arginine at amino acid 249; and 4) G245S, identified from a Li-Fraumeni family with a high breast cancer incidence. In addition, we have made the empty viral vector and a GFP containing vector for use as infection controls.

Task 7 – Transfection and monitoring experiments (months 35-46). This Task has recently been initiated. We are very encouraged by our initial results using viral vectors for the R195* and C238F mutant vectors and the 2 control vectors. We have not yet used the R249G or G245S mutant vectors. After only 48 hours post transduction, 80% of the mitotic cells expressing the R195* mutant p53 had multipolar spindles. This phenotype correlates with the phenotype of high chromosomal instability and numerous centrosomes of the tumor in which this mutation was identified. None of the mitotic cells expressing the C238F mutant p53 had multipolar spindles. This also correlates with the phenotype of

the tumor in which this mutant was identified. This tumor had normal centrosome size and number and a stable, but aneuploid karyotype. The frequency of abnormal mitoses in the control cells was near zero.

Task 8 – Data analysis and manuscript preparation (months 38-48). To date, 3 original research papers have been published from work supported by this grant (Appendices I - III). We expect to publish one or more papers from the research contained in Task 7.

KEY RESEARCH ACCOMPLISHMENTS

- Excess pericentriolar material is a specific centrosome defect associated with an increased frequency of abnormal mitoses in human breast tumors.
- A specific p53 mutation (glycine to serine at amino acid 245) induces abnormal centrosome structure and function upon transfection of primary normal human mammary epithelial cells.
- Tumor aneuploidy correlates with centrosome amplification.
- Centrosome number and centrosome size each have a statistically significant linear correlation with chromosomal instability.
- Centrosome microtubule nucleation capacity does not correlate with chromosomal instability.
- Centrosome microtubule nucleation capacity does correlate with loss of tumor differentiation.
- Tumors with p53 mutations have a statistically significant 2 fold higher capacity to nucleate microtubules than tumors with wild type p53.
- p53 mutations have been identified in breast tumors that are associated with centrosome amplification and aneuploidy.
- Specific p53 mutations have different effects on centrosome function.

REPORTABLE OUTCOMES

Invited Seminars

1. Aberrant Structure and Function of Centrosomes in Human Breast Tumors. March 1999 GI Unit Scientific Meeting, Mayo Clinic, Rochester, MN.
2. Breast Cancer: Centrosomes, Aneuploidy, and Progression. February 2000. University of Puerto Rico Medical School, San Juan, PR.
3. Aberrant Structure and Function of Centrosomes in Breast Cancer. June 2000. Department of Cellular Biology, University of Georgia, Athens, GA.
4. Centrosomes, Aneuploidy, and Breast Cancer. 2000. Mayo Laboratory Society, Mayo Clinic, Rochester, MN.
5. Chromosomal Instability Correlates with Centrosome Amplification in Human Breast Cancer. June 2001. GI Research Seminar Series. Mayo Clinic, Rochester, MN.
6. The Role of the Centrosome in Development and Progression of Breast Cancer. August 2001. Invited Speaker in "Biology of Cancer" Symposium at the Annual Meeting of the Microscopy Society of America. Long Beach, California.
7. Centrosome Amplification Drives Chromosomal Instability in Breast Tumor Development. 2001. Chromosomal Instability and DNA Damage Interest Group.
8. Centrosome Amplification Drives CIN in Breast Tumor Development. 2001. Experimental Pathology Research Seminar Series.

Publications

1. Salisbury, JL, Whitehead, CM, **Lingle, WL**, and Barrett, SL. 1999. Centrosomes and cancer. Biology of the Cell. 91:451-460.
2. Salisbury, JL, **Lingle, WL,** White, RA, Cordes, LEM, and Barrett, SL. 1999. A simple method to assess microtubule nucleating capacity of centrosomes in tissue sections. J. Histochem. Cytochem. 47:1265-1273.
3. **Lingle, WL** and Salisbury, JL. 1999. Altered centrosome structure in human breast tumors. American J. Pathol. 155:1941-1951. **Cover photo**.
4. **Lingle, WL** and Salisbury, JL. 2000. The role of the centrosome in the development of malignant tumors. In: The centrosome in reproduction and cell replication (Palazzo, RE, ed). Current Topics in Developmental Biology, Academic Press. 49:313-329.
5. Lutz, W, **Lingle, WL**, McCormick, D, Greenwood, TM, and Salisbury, JL. 2001. Phosphorylation of centrin during the cell cycle and its role in centriole separation preceding centrosome duplication. J. Biological Chemistry. 276:20774-20780.
6. **Lingle, WL** and Salisbury, JL. 2001. Microtubule nucleation assay to measure centrosome amplification in tissues. In: Methods in Cell Biology, Centrosome in Cell Replication and Early Development (Palazzo, RE, ed). Academic Press. 67:331-342.
7. **Lingle, WL**, Barrett, SL, Negron, VC, D'Assoro, AB, Boeneman K, Liu, W, Whitehead, CM, Reynolds C, Salisbury, JL. 2002. Centrosome amplification drives chromosomal instability in breast tumor development. PNAS. 99: 1978-1983. **Featured in "Highlights in Brief" in Nature Reviews Cancer 2, 155 (01 Mar 2002).**

18. D'Assoso, A, Barrett, SL, Folk, C, Negron, CV, Boeneman, K, Busby, R, Whitehead, CM, Stivala, F, **Lingle, WL**, and Salisbury, JL. 2002. *In Press.* Centrosome amplification is a marker for genomic instability in breast cancer cell lines with diverse phenotypes. Breast Cancer Research and Treatment.

Research Funding Received On The Basis Of Work Supported By This Award

DAMD 17-01-1-0753 (**Lingle**, PI) 8/1/01 – 7/31/04 25%
DoD Breast Cancer Research Program $391,521
"Investigation of gene expression correlating with centrosome amplification in development and progression of breast cancer"

Eagles' Award (**Lingle**, PI) 07/01/01 – 06/30/02
Mayo Clinic Internal Cancer Research Program $30,000
"Effects of Mutant p53 on the Structure and Function of Centrosomes and the Mitotic Spindle Apparatus"

Breast Cancer Center of Excellence Award 1/02 - 12/05 10%
(Hartmann, PI; **Lingle**, CoI)
DoD Breast Cancer Research Program $4,000,000
"Benign Breast Disease: Toward the Molecular Prediction of Breast Cancer Risk"

Promotion received on the basis of experience supported by this award

Senior Research Fellow to Associate Consultant, effective March 1, 1999.

CONCLUSIONS

To date, the research supported by this award has yielded results with significant implications regarding the origin and perpetuation of aneuploidy in breast cancer, especially related to centrosome amplification and p53 mutation. First, excess pericentriolar material has been linked with an increased frequency of abnormal mitoses in tumor tissues. This demonstrates that at least one aspect of centrosome amplification is associated with mitotic events that most often result in aneuploid daughter cells. Furthermore, the increase in amplified centrosomes and abnormal mitoses was duplicated in limited *in vitro* studies. In these studies, cultured normal mammary epithelial cells were transfected with G245S mutant p53; indicating that **p53 mutation may be involved in centrosome amplification associated with abnormal mitoses that can lead to aneuploidy.**

A second important result demonstrated the correlation of aneuploidy with centrosome amplification in breast tumors using fluorescence in situ hybridization with centromeric probes to chromosomes 3, 7, and 17. In these studies, 18 of 21 tumors were found to be aneuploid while three were diploid. The three diploid tumors had nearly normal centrosomes, while all 18 aneuploid tumors displayed centrosome amplification. **Further analysis revealed a statistically significant linear correlation between chromosomal instability and centrosome number and centrosome size. However, there was no correlation between the microtubule nucleation capacity of tumor centrosomes and chromosomal instability.** Microtubule nucleation capacity of tumors does show a correlation with loss of tissue differentiation as determined by the Nottingham Grading system. The less differentiated Grade II and III tumors had significantly greater microtubule nucleation capacity than the more differentiated Grade I tumors, and all grades were significantly greater than fully differentiated normal tissues. **Together, these results indicate that different aspects of centrosome amplification have different effects on tumor progression. Centrosome size and number affect chromosomal instability, while microtubule nucleation capacity affects cell, and therefore, tissue architecture. Chromosome instability has profound implications for tumor progression, while changes in cell architecture can increase metastatic potential.**

Third, on average, centrosome of tumors with p53 mutations had a 2 fold greater capacity to nucleate microtubules than centrosomes from tumors with wild type p53. The two other measures of centrosome amplification used in this study, centrosome size and centrosome number, were not significantly different between the two groups. **In light of the conclusions from the previous paragraph, this means that mutations in p53 may increase tumor grade by affecting the microtubule cytoskeleton of the tumor cells. Initial experiments using adenoviral vectors containing 2 different p53 mutations indicate that specific p53 mutations have different effects on centrosome function.**

APPENDICES

Appendix I - Lingle, WL and Salisbury, JL. 1999. Altered centrosome structure in human breast tumors. American J. Pathol. 155:1941-1951.

Appendix II - D'Assoso, A, Barrett, SL, Folk, C, Negron, CV, Boeneman, K, Busby, R, Whitehead, CM, Stivala, F, **Lingle, WL**, and Salisbury, JL. 2002. *In Press.* Amplified centrosomes in breast cancer: A potential indicator of tumor aggressiveness. Breast Cancer Research and Treatment.

Appendix III - Lingle, WL, Barrett, SL, Negron, VC, D'Assoro, AB, Boeneman K, Liu, W, Whitehead, CM, Reynolds C, Salisbury, JL. 2002. Centrosome amplification drives chromosomal instability in breast tumor development. PNAS. 99: 1978-1983.

Running Head: Centrosome amplification in breast tumors

Article type: Article

Amplified Centrosomes In Breast Cancer: A Potential Indicator Of Tumor Aggressiveness

Antonino B. D'Assoro[1], Susan L. Barrett[1], Christopher Folk[1], Vivian C. Negron[1], Kelly Boeneman[1], Robert Busby[1], Clark Whitehead[1], Franca Stivala[4], Wilma L. Lingle[1,2,3] and Jeffrey L. Salisbury[1,3]

[1]Tumor Biology Program, [2]Experimental Pathology, Mayo Clinic Foundation, Rochester, MN 55905 and [4] Institute of General Pathology, University of Catania, Italy 95123

[3]Both laboratories contributed equally to this work.

Correspondence should be addressed to W.L.L. or J.L.S.

Email: lingle.wilma@mayo.edu

salisbury@mayo.edu

Manuscript correspondence: Jeffrey L. Salisbury, Tumor Biology Program, Mayo Clinic Foundation, Rochester, MN 55905. email: salisbury@mayo.edu

Running title: **Centrosome Amplification in Breast Cancer**

Key Words: estrogen receptor, p53, $p21^{Waf1/Cip1}$, aneuploidy, microtubules, mitotic spindle

Summary

Molecular mechanisms leading to genomic instability and phenotypic variation during tumor development and progression are poorly understood. Such instability represents a major problem in the management of breast cancer because of its contribution to more aggressive phenotypes as well as chemoresistence. In this study we analyzed breast carcinomas and tumor-derived cell lines to determine the relationship between centrosome amplification and established prognostic factors. Our results show that centrosome amplification can arise independent of ER or p53 status and is a common feature of aneuploid breast tumors. Centrosome amplification is associated with mitotic spindle abnormalities in breast carcinomas and thus may contribute to genomic instability and the development of more aggressive phenotypes during tumor progression.

INTRODUCTION

Breast cancer, like most other cancers, is characterized by complex and heterogeneous genetic alterations originating from genomic instability and aneuploidy [1]. Genomic instability leads to the persistent generation of new chromosomal variations, to tumor progression and to the development of more aggressive phenotypes with increased metastatic potential and chemoresistence [2]. The steroid hormone estradiol plays an important role in the etiology of breast cancer [3]. Often, breast tumors progress from a hormone-dependent to a more aggressive hormone-independent phenotype [4]. Hormone-independent tumors are less likely to be well differentiated, are aneuploid and in general show more frequent mutations, including loss or amplification of breast cancer related genes (p53, ErbB2/HER-2/neu, EGFR) [5]. For this reason, the hormone responsive status of breast tumors is considered one of the most important prognostic factors for predicting clinical outcome, and so is used to determine appropriate treatment for breast cancer patients.

Centrosome defects are characteristic of breast cancer and solid tumors in general [6-11]. The centrosome plays an essential role in equal segregation of chromosomes through the

establishment of the bipolar mitotic spindle. Precise control of centrosome duplication is strictly coordinated with DNA replication during cell cycle progression. In cancer cells, alteration of centrosome homeostasis by disregulation of cell cycle checkpoints leads to centriole over-duplication and multipolar mitoses, thereby increasing the rate of chromosomal instability. Interestingly, loss of function of the tumor suppressor gene p53 leads to centrosome amplification and aneuploidy [7, 12-15]. The mechanism for p53 control of centrosome duplication is probably mediated, in part, through transcriptional regulation of the cyclin-dependent kinase inhibitor $p21^{Waf1/Cip1}$ and its subsequent inhibition of Cdk/cyclin D and E activity [16-19]. GADD45, another component of the p53 pathway, has also been implicated in the maintenance of genomic stability through regulation of centrosome homeostasis [20].

In this study we analyzed centrosome characteristics in breast carcinomas and tumor derived cell lines with different phenotypes to clarify the relationship between centrosome amplification and estrogen receptor (ER), ErbB2, EGFR and $p21^{Waf1/Cip1}$ expression, p53 status, mitotic abnormalities and metastatic potential. Our studies reveal three important points: 1) tumor derived cell lines show a range of centrosome phenotypes and increased centrosome amplification correlates with tumor aggressiveness, 2) centrosome amplification can arise independent of ER or p53 status, and 3) centrosome amplification is linked to chromosomal instability. -Based on these observations we propose that centrosome amplification could play a key role in the development of phenotypic variation through increased genomic instability.

MATERIALS AND METHODS

Human tissue samples and cell culture. Human breast tissue was obtained immediately after surgery according to an IRB approved protocol, frozen in liquid nitrogen and stored at –70 C° until use. For electron microscopy fresh tissue was processed immediately in Trumps fixative according to [21]. Specimens were obtained from patients who had no chemotherapeutic or radiation treatments before surgery. Human breast cancer cell lines were obtained from ATCC. MCF-7 and T-47D cells were grown in RPMI 1640 medium,

and MDA-MB231 cells were grown in MEM medium supplemented with 2mM L-glutamine, 1% penicillin/streptomycin and 10% fetal bovine serum in 5% CO_2 in air at 37° C.

Microtubule nucleation assay. Breast cancer cell lines grown on glass cover slips and cryosections of breast tissue were processed as described earlier [22, 23]. The number of microtubules nucleated per cell was counted for 100 consecutively viewed cells. Earlier studies demonstrated that this assay clearly distinguishes mitotic and interphase microtubule nucleation capacity of cultured cells [23]. The study reported here for the cell lines was conducted on sub-confluent cultures plated 24 hrs prior to microtubule nucleation and the analysis was restricted to interphase cells (only cells with a single centrosome were counted). Cells with significant overlap of microtubule arrays were excluded from analysis, as were obviously damaged cells. Microtubule nucleation capacity is reported as the *MT Index* = average # microtubules nucleated by the experimental specimen (n=50) divided by the average # microtubules nucleated by the control specimen (n=50). For MT Index of cell lines, normal human mammary epithelial cell cultures (HMEC, Clonetics, Walkersville, MD) were used as controls. The MT Index for tissues was determined against the average value for 5 separate normal mammary epithelial tissue specimens set as the normalized control value.

Microscopy and Western analyses. Antibodies used for indirect immunofluorescence and Western analysis were obtained from the following sources: β-actin, α-tubulin, γ-tubulin, ER (Sigma, St. Louis, MO), pericentrin (Babco, Richmond, CA), p53 (DAKO, Mississauga, ON, Canada), ErbB2 (Santa Cruz, Santa Cruz, CA), EGFR (Genosys, The Woodland, TX), and $p21^{Waf1/Cip1}$ (Oncogene, Boston, MA), centrin (20H5, our laboratory), and HsEg5 (a generous gift from Dr. JB Rattner [24]). For indirect immunofluorescence the primary antibodies were followed by FITC, Alexa 488, Alexa 568 (Molecular Probes, Eugene, OR), or rhodamine-conjugated secondary antibodies and Hoechst 33342 stain for DNA.

Methods for indirect immunofluorescence and Western analysis were carried out as described earlier [9]. Centrosome volume was determined using quantitative confocal microscopy for two different centrosome proteins (centrin and pericentrin) [9]. Centrosome number and volume per nucleus in cell lines and in tumor and adjacent 'normal' tissue were determined and assessed to measure specimen variability. The median value of the number and volume of centrosomes per nucleus for tumor and normal tissue was used as a summary statistic. Immunofluorescence analyses were preformed using either a Zeiss LSM 510 high resolution laser confocal microscope or a Nikon FXA fluorescence microscope equipped with computer controlled focus, CCD digital camera, and MetamorphTM (Universal Imaging Corp) software. Fields were recorded at multiple focal planes to assure that all centrioles and centrosomal structures were imaged. Images were analyzed and printed as maximum projections. Spindle morphology was scored as normal 'bipolar' if less than 1% aberrant spindles were present (n = 100 spindles). Mitotic figures in the normal breast tissue were extremely rare, however in the several instances where they were found they were bipolar. Centriole numbers were determined by counting immunofluorescence anti-centrin stained spots in 100 cells. Centrosome volume measurements for breast tumors were made using confocal microscopy and volume reconstructions as described earlier [9, 25]. A "Normal Centrosome" phenotype was defined as two or four centrioles per cell and a calculated centrosome volume based on total centrin staining of between 0.015 and 0.075 μm^3. An "Amplified Centrosome" phenotype was defined as more than four centrioles per cell and/or a centrosome volume greater than 0.075 μm^3. For Western blots, cell lysates (50 µg) were separated by SDS/PAGE, transferred to PVDF membranes (Millipore, Bedford, MA), reacted with appropriate antibody followed by HRP-conjugated secondary, and visualized by chemiluminescence using ECL reagents according to manufacturer's instructions (Amersham, Piscataway, NJ).

FISH probes to pericentromeric regions of chromosomes 3 (CEP3), 7 (CEP7), and 17 (CEP17) (Vysis, Inc., Downers Grove, IL) were hybridized to touch preparations of nuclei from frozen tissues according to previously published methods [26, 27]. Probes

were labeled with SpectrumOrange™ (CEP3), SpectrumGreen™ (CEP7), and SpectrumAqua™ (CEP17) for simultaneous analysis. DNA was counterstained with DAPI prior to mounting coverslips. For each tissue, 100 consecutive nuclei were scored for the number of signals for each of the three probes per nucleus using methods described previously [28]. Classification of tissue ploidy was a two-step process. In the first step, each of the 100 cells for a given tissue was classed either as disomic if all 3 probes had 2 signals, as polysomic if 2 or more probes had more than 2 signals, as monosomic for a given probe, or otherwise as non-disomic. For the second step, the sum of the cells in each of the above categories was used to determine the tissue status as follows: 1) diploid if at least 50% of the cells were disomic, fewer than 15% were polysomic, and fewer than 50% were monosomic for the same chromosome, or 2) aneuploid if more than 15% of the cells were polysomic. Results from the 7 reduction mammoplasties (assumed to be diploid) were used to calculate these cutoff values.

Statistical Analysis. Significance of differences in centrosome size, number, and MT nucleation capacity, or wild-type or mutant p53 was determined using the Wilcox rank sum test.

Analysis of p53 and estrogen receptor status. For the indirect fluorescence determinations, p53 mutations were scored as positive if more than 40% of the tumor cell nuclei in four fields of 400X label intensely with anti-p53 monoclonal antibody. In addition, breast tissue p53 mutations were determined by denaturing high performance liquid chromatography of PCR products [29] for detection of mutations in exons 4-9 and confirmed by subsequent sequencing for all tumor samples. Estrogen receptor status was determined using an immunohistochemistry-based assay [30].

RESULTS

Centrosome phenotypes, estrogen dependence, p53 status and metastatic potential in breast cancer cell lines. For *in vitro* studies, we used three human breast cancer cell lines (MCF-7, T-47D, and MDA-MB231) to investigate the relationship between centrosome amplification and established prognostic markers of breast cancer. Centrosome amplification was assessed by both structural and functional criteria. For these studies the number of centrioles and the amount of the surrounding pericentriolar material (PCM) were determined using immunofluorescence for centrin and pericentrin, respectively. Centrosome function was determined using a quantitative assay for microtubule nucleation and mitotic spindle morphology. The three cell lines can be ordered according to increasing centrosome amplification as determined by the percentage of cells showing excess (>4) centriole number and microtubule nucleation capacity (Table I, Fig. 1). The breast tumor cell line MCF-7 showed normal appearing centrosomes with two or four centrin staining spots (centrioles) surrounded by a moderate amount of PCM (Fig. 1, Table I). In contrast, the breast tumor cell lines T-47D, and MDA-MB231 showed centrosome amplification characterized by multiple centrin staining spots (supernumerary centrioles) and excess PCM (Fig 1, Table I). Since tumor centrosomes are typified by alterations in microtubule nucleation [8, 9], we performed a functional assay to determine microtubule nucleation capacity on detergent extracted models of the three breast cancer cell lines. These studies revealed that increased microtubule nucleation reflected centrosome amplification (Fig. 1, Table I). Similarly, the three cell lines displayed a range of mitotic spindle abnormalities reflecting the status of genomic instability (Fig. 1 d and Table I). Each of the cell lines showed the majority of dividing cells with normal mitotic figures. Nonetheless, MCF-7 cells showed 10% abnormal mitoses, and T-47D, and MDA-MB231 showed a higher frequency (14 and 22%, respectively) of aberrant mitoses, including multipolar spindles, lagging chromosomes and cytokinesis defects.

These same three human breast tumor cell lines were assessed for ER, ErbB2, EGFR, and $p21^{Waf1/Cip1}$ expression and p53 mutation status. The estrogen-dependent cell lines MCF-7

and T-47D both show ER expression by Western analysis, while the estrogen-independent cell line MDA-MB231 lacks ER entirely (Fig. 2). As described earlier [31], each of these cell lines showed a distinctive growth factor receptor expression pattern. ErbB2 expression was found in each cell line and was highest in T-47D. In contrast, EGFR expression was high in the MDA-MB231, low in T-47D, and undetectable in MCF-7 cell lines (Fig. 2). MCF-7, with a wild-type p53 phenotype [32], showed no detectable p53 (Fig. 2), whereas T-47D, and MDA-MB231 cell lines, which have been reported to express mutant p53, showed high levels of p53 accumulation that was largely localized in the nucleus (Fig. 2). Expression analysis also showed a high level of expression of the cdk/cyclin inhibitor $p21^{Waf1/Cip1}$, a downstream effector of the p53 pathway, in MCF-7 and T-47D, and low levels in MDA-MB231 cells (Fig. 2). The metastatic potential of the three cell lines has been determined in nude mice [33, 34], and in this model system MCF-7 shows the least aggressive behavior, with increasing metastatic potential observed for T-47D, MDA-MD231, respectively [35, 36]. Table I summarizes the characteristics of the three breast cancer cell lines in relation to centrosome phenotype. Taken together, these results demonstrate that centrosome amplification in tumor derived cell lines is associated with loss of estrogen-dependence and p53 function, over expression of EGF receptor, mitotic abnormalities and demonstrated metastatic potential.

Centrosome amplification and aneuploidy in breast tumors. For studies on human breast tissue we analyzed seven normal breast tissues and sixteen invasive breast tumor specimens for centrosome amplification, aberrant mitoses, DNA ploidy, ER, p53, and lymph node status (Fig. 3 and Table I). From these tumor tissues, distinct phenotypes were recognized, three of which matched the phenotypes of the breast cancer cell lines described above (Fig. 3 b-d and Table I). Like the human breast cancer cell lines, the tumors could be arranged according to increasing centrosome amplification based on centrin and pericentrin staining (Table I). In these breast tumors, the level of centrosome amplification also reflected the degree of aneuploidy based on FISH analysis of chromosomes 3, 7 and 17, where diploid tumors showed nearly normal centrosomes and aneuploid tumors showed centrosome amplification. Several important findings emerged

from these studies. Diploid breast tumors consistently displayed normal centrosomes, bipolar mitotic spindle morphology, and were both positive for ER and wild type p53, whereas all aneuploid tumors showed amplified centrosomes, and higher levels of mitotic abnormalities. Finally, the most severe examples of centrosome amplification occurred in more aggressive tumor phenotypes based on lymph node status (Table I). These observations confirm the correlation between centrosome amplification with an increase in mitotic abnormalities (9, 20) and demonstrate a relationship with aneuploidy, and tumor aggressiveness (Figs. 3, Table I).

Ultrastructural analysis of centrosomes in breast carcinomas and tumor derived cell lines. Analysis at the electron microscope established the ultrastructure of centrosomes in these tumors and cell lines (Fig. 4). Centrosomes containing two centrioles and nominal PCM were characteristic of epithelial cells of normal breast tissue and diploid tumors, and also of the normal human mammary epithelial (HMEC) and MCF-7 cell lines (Figs. 4 a-b and e-f). In contrast, centrosome defects, characterized by centriole over-duplication, were observed in aneuploid breast tumors and in the aneuploid cell line MDA-MB231 (Figs. 4 c-d and g). These studies confirm the fluorescence microscopy observations reported above where diploid and near-diploid breast tissues and cell lines displayed normal centrosome structure and function, whereas aneuploid tumors show gross structural alterations in amplified centrosomes. We reported earlier that breast tumors with excess PCM show a higher number of abnormal mitoses [21].

DISCUSSION

Cancer progression occurs through accumulation of genetic alterations, cancer cell heterogeneity and, ultimately, the development of more aggressive phenotypes. Since established prognostic parameters such as tumor size, lymph node status, histologic grade and hormone receptor status do not precisely predict outcome, there is a need for new prognostic markers with increased predictive value. DNA ploidy reflects an aspect of genomic instability and is often associated with grade of differentiation, ER and p53 status and ErbB2 over-expression [37-39]. Diploid tumors are generally less aggressive

and have a more favorable outcome than aneuploid tumors [40]. The precise control of centrosome duplication during cell cycle progression ensures equal chromosome segregation, which is critical in maintenance of diploid status. Positive and negative cell cycle regulators, such as Cdk2/cyclin E, p53, Rb, BRCA1, BRCA2 and $p21^{Waf1/Cip1}$, are also involved in the control of centrosome duplication [17, 18, 41-46]. They are likely the molecular targets linking deregulation of cell cycle checkpoints with centrosome amplification and development of chromosomal instability during tumor development and progression [47]. Our studies demonstrate that breast carcinomas and tumor-derived cell lines show centrosome amplification that may drive chromosomal instability. Therefore, centrosome amplification might also reflect consequent development of clonal heterogeneity in a tumor cell population and thereby increase their potential for developing metastasis. Selection from the resulting heterogeneous cell population can promote more aggressive phenotypes and chemoresistance. These relationships may be common for solid tumors in general since others have drawn similar conclusions for prostate, pancreatic and colorectal cancer [8, 48, 49]. Our analysis suggests that centrosome amplification in breast cancer may be a consequence of an imbalance between oncogenes and tumor suppressors. For example, inactivation of p53, loss of ER, and overexpression of EGFR during tumor progression may represent common mechanisms which result in the acceleration of chromosomal instability by uncoupling centrosome duplication from the cell cycle. Interestingly, in tumor derived cell lines, $p21^{Waf1/Cip1}$, a down stream effector of the p53 pathway may be involved with control of centrosome homeostasis and tumor aggressiveness through its role in regulation of the G1/S cell cycle checkpoint [41, 50, 51]. However, while loss of p53 function and ER may play an important role in the development of centrosome over duplication, centrosome amplification was also present in ER positive tumors with wild type p53 (Table I). Therefore, mechanisms independent of ER and p53 status may also contribute to the induction of centrosome amplification in breast cancer.

The study reported here suggests that centrosome amplification might be useful in monitoring chromosomal instability and in turn phenotypic diversity in breast cancer. For example, based on the status of centrosome phenotype, hormone responsive and

lymph node negative patients may be stratified into two groups, those that require only endocrine treatment and those that require more aggressive treatment due to increased chromosomal instability associated with centrosome amplification. Finally, in association with other established prognostic factors, centrosome amplification may be helpful in predicting outcomes and survival of patients with breast cancer.

ACKNOWLEDGEMENTS

This work was supported by NCI CA72836 to JLS, DAMD 17-98-1-8222 to WLL, by the University of Catania Italy to ABD and the Mayo Foundation.

REFERENCES

1. Lengauer, C, Kinzler, KW Vogelstein, B: Genetic instabilities in human cancers. Nature 396: 643-649., 1998

2. Loeb, LA: A Mutator Phenotype in Cancer. Cancer Res 61: 3230-3239, 2001

3. Russo, J, Hu, Y-F, Yang, X. Russo, IH: Developmental, cellular, and molecular basis of human breast cancer. J. Natl. Cancer Instit. Monographs 27: 17-37, 2000

4. Khan, SA, Rogers, MA, Khurana, KK, Meguid, MM Numann, PJ: Estrogen receptor expression in benign breast epithelium and breast cancer risk. J Natl Cancer Inst 90: 37-42., 1998

5. Thor, A Yandell, D: Molecular Pathology of Breast Carcinoma. In: J. Harris, M. Lippman, M. Morrow and S. Hellman (eds) Diseases of the Breast. Lippincott-Raven, Philadelphia, 1996, pp 445-454

6. Brinkley, BR: Managing the centrosome numbers game: from chaos to stability in cancer cell division. Trends Cell Biol 11: 18-21., 2001

7. Carroll, PE, Okuda, M, Horn, HF, Biddinger, P, Stambrook, PJ, Gleich, LL, Li, YQ, Tarapore, P Fukasawa, K: Centrosome hyperamplification in human cancer: chromosome instability induced by p53 mutation and/or Mdm2 overexpression. Oncogene 18: 1935-1944, 1999

8. Ghadimi, BM, Sackett, DL, Difilippantonio, MJ, Schrock, E, Neumann, T, Jauho, A, Auer, G Ried, T: Centrosome amplification and instability occurs exclusively in aneuploid, but not in diploid colorectal cancer cell lines, and correlates with numerical chromosomal aberrations. Genes Chromosomes Cancer 27: 183-190, 2000

9. Lingle, WL, Lutz, WH, Ingle, JN, Maihle, NJ Salisbury, JL: Centrosome hypertrophy in human breast tumors: implications for genomic stability and cell polarity. Proc Natl Acad Sci U S A 95: 2950-2955, 1998

10. Pihan, GA, Purohit, A, Wallace, J, Knecht, H, Woda, B, Quesenberry, P Doxsey, SJ: Centrosome defects and genetic instability in malignant tumors. Cancer Res 58: 3974-3985, 1998

11. Zhou, H, Kuang, J, Zhong, L, Kuo, WL, Gray, JW, Sahin, A, Brinkley, BR Sen, S: Tumour amplified kinase STK15/BTAK induces centrosome amplification, aneuploidy and transformation. Nat Genet 20: 189-193, 1998

12. Duensing, S, Duensing, A, Crum, CP Munger, K: Human Papillomavirus Type 16 E7 Oncoprotein-induced Abnormal Centrosome Synthesis Is an Early Event in the Evolving Malignant Phenotype. Cancer Res 61: 2356-2360, 2001

13. Fukasawa, K, Choi, T, Kuriyama, R, Rulong, S Vande Woude, GF: Abnormal centrosome amplification in the absence of p53. Science 271: 1744-1747, 1996

14. Murphy, KL, Dennis, AP Rosen, JM: A gain of function p53 mutant promotes both genomic instability and cell survival in a novel p53-null mammary epithelial cell model. Faseb J 14: 2291-2302., 2000

15. Wang, XJ, Greenhalgh, DA, Jiang, A, He, D, Zhong, L, Brinkley, BR Roop, DR: Analysis of centrosome abnormalities and angiogenesis in epidermal- targeted p53172H mutant and p53-knockout mice after chemical carcinogenesis: evidence for a gain of function. Mol Carcinog 23: 185-192, 1998

16. Hinchcliffe, EH, Miller, FJ, Cham, M, Khodjakov, A Sluder, G: Requirement of a centrosomal activity for cell cycle progression through G1 into S phase. Science 291: 1547-1550., 2001

17. Lacey, KR, Jackson, PK Stearns, T: Cyclin-dependent kinase control of centrosome duplication. Proc Natl Acad Sci U S A 96: 2817-2822, 1999

18. Mantel, C, Braun, SE, Reid, S, Henegariu, O, Liu, L, Hangoc, G Broxmeyer, HE: p21(cip-1/waf-1) deficiency causes deformed nuclear architecture, centriole overduplication, polyploidy, and relaxed microtubule damage checkpoints in human hematopoietic cells. Blood 93: 1390-1398, 1999

19. McShea, A, Samuel, T, Eppel, JT, Galloway, DA Funk, JO: Identification of CIP-1-associated regulator of cyclin B (CARB), a novel p21-binding protein acting in the G2 phase of the cell cycle. J Biol Chem 275: 23181-23186, 2000

20. Hollander, MC, Sheikh, MS, Bulavin, DV, Lundgren, K, Augeri-Henmueller, L, Shehee, R, Molinaro, TA, Kim, KE, Tolosa, E, Ashwell, JD, Rosenberg, MP, Zhan, Q, Fernandez-Salguero, PM, Morgan, WF, Deng, CX Fornace, AJ, Jr.: Genomic instability in Gadd45a-deficient mice. Nat Genet 23: 176-184, 1999

21. Lingle, WL Salisbury, JL: Altered centrosome structure is associated with abnormal mitoses in human breast tumors. Am J Pathol 155: 1941-1951, 1999

22. Lingle, WL Salisbury, JL: Methods for the analysis of centrosome reproduction in cancer cells. Methods Cell Biol 67: 325-336, 2001

23. Salisbury, JL, Lingle, WL, White, RA, Cordes, LE Barrett, S: Microtubule nucleating capacity of centrosomes in tissue sections. J Histochem Cytochem 47: 1265-1274, 1999

24. Whitehead, CM, Winkfein, RJ Rattner, JB: The relationship of HsEg5 and the actin cytoskeleton to centrosome separation. Cell Motil Cytoskeleton 35: 298-308, 1996

25. Lingle, WL, Barrett, SL, Negron, VC, D'Assoro, AB, Boeneman, K, Liu, W, Whitehead, CM, Reynolds, C Salisbury, JL: Centrosome amplification drives chromosomal instability in breast tumor development. Proc Natl Acad Sci U S A (in press): 2001

26. Halling, KC, King, W, Sokolova, IA, Meyer, RG, Burkhardt, HM, Halling, AC, Cheville, JC, Sebo, TJ, Ramakumar, S, Stewart, CS, Pankratz, S, O'Kane, DJ, Seelig, SA, Lieber, MM Jenkins, RB: A comparison of cytology and fluorescence in situ hybridization for the detection of urothelial carcinoma. J Urol 164: 1768-1775., 2000

27. Persons, DL, Robinson, RA, Hsu, PH, Seelig, SA, Borell, TJ, Hartmann, LC Jenkins, RB: Chromosome-specific aneusomy in carcinoma of the breast. Clin Cancer Res 2: 883-888., 1996

28. Sokolova, IA, Halling, KC, Jenkins, RB, Burkhardt, HM, Meyer, RG, Seelig, SA King, W: The development of a multitarget, multicolor fluorescence in situ hybridization assay for the detection of urothelial carcinoma in urine. J Mol Diagn 2: 116-123., 2000

29. Liu, W, Smith, DI, Rechtzigel, KJ, Thibodeau, SN James, CD: Denaturing high performance liquid chromatography (DHPLC) used in the detection of germline and somatic mutations. Nucleic Acids Res 26: 1396-1400., 1998

30. King, WJ Greene, GL: Monoclonal antibodies localize oestrogen receptor in the nuclei of target cells. Nature 307: 745-747., 1984

31. deFazio, A, Chiew, YE, Sini, RL, Janes, PW Sutherland, RL: Expression of c-erbB receptors, heregulin and oestrogen receptor in human breast cell lines. Int J Cancer 87: 487-498., 2000

32. Wosikowski, K, Regis, JT, Robey, RW, Alvarez, M, Buters, JT, Gudas, JM Bates, SE: Normal p53 status and function despite the development of drug resistance in human breast cancer cells. Cell Growth Differ 6: 1395-1403., 1995

33. Price, JE: Metastasis from human breast cancer cell lines. Breast Cancer Res Treat 39: 93-102, 1996

34. Clarke, R, Leonessa, F, Brünner, WN Thompson, EW: *In Vitro* Models. In: J. R. Harris (eds) Diseases of the Breast. Lippincott Williams, Philadelphia, 2000, pp 335-354

35. Keydar, I, Chen, L, Karby, S, Weiss, FR, Delarea, J, Radu, M, Chaitcik, S Brenner, HJ: Establishment and characterization of a cell line of human breast carcinoma origin. Eur J Cancer 15: 659-670., 1979

36. Soule, HD, Vazguez, J, Long, A, Albert, S Brennan, M: A human cell line from a pleural effusion derived from a breast carcinoma. Journal of the National Cancer Institute 51: 1409-1416, 1973

37. Anbazhagan, R, Gelber, RD, Bettelheim, R, Goldhirsch, A Gusterson, BA: Association of c-erbB-2 expression and S-phase fraction in the prognosis of node positive breast cancer. Ann Oncol 2: 47-53., 1991

38. Wenger, CR, Beardslee, S, Owens, MA, Pounds, G, Oldaker, T, Vendely, P, Pandian, MR, Harrington, D, Clark, GM McGuire, WL: DNA ploidy, S-phase, and steroid receptors in more than 127,000 breast cancer patients. Breast Cancer Res Treat 28: 9-20., 1993

39. Gunther, T, Schneider-Stock, R, Rys, J, Niezabitowski, A Roessner, A: p53 gene mutations and expression of p53 and mdm2 proteins in invasive breast carcinoma. A comparative analysis with clinico-pathological factors. J Cancer Res Clin Oncol 123: 388-394, 1997

40. O'Reilly, SM, Camplejohn, RS, Barnes, DM, Millis, RR, Allen, D, Rubens, RD Richards, MA: DNA index, S-phase fraction, histological grade and prognosis in breast cancer. Br J Cancer 61: 671-674., 1990

41. Hinchcliffe, EH, Li, C, Thompson, EA, Maller, JL Sluder, G: Requirement of Cdk2-cyclin E activity for repeated centrosome reproduction in Xenopus egg extracts. Science 283: 851-854., 1999

42. Hsu, LC White, RL: BRCA1 is associated with the centrosome during mitosis. Proc Natl Acad Sci U S A 95: 12983-12988, 1998

43. Meraldi, P, Lukas, J, Fry, A, Bartek, J Nigg, E: Centrosome duplication in mammalian somatic cells requires E2F and Cdk2-cyclin A. Nature Cell Biol 1: 88-93, 1999

44. Mussman, JG, Horn, HF, Carroll, PE, Okuda, M, Tarapore, P, Donehower, LA Fukasawa, K: Synergistic induction of centrosome hyperamplification by loss of p53 and cyclin E overexpression. Oncogene 19: 1635-1646, 2000

45. Xu, X, Weaver, Z, Linke, SP, Li, C, Gotay, J, Wang, XW, Harris, CC, Ried, T Deng, CX: Centrosome amplification and a defective G2-M cell cycle checkpoint induce genetic instability in BRCA1 exon 11 isoform-deficient cells. Mol Cell 3: 389-395, 1999

46. Tutt, A, Gabriel, A, Bertwistle, D, Connor, F, Paterson, H, Peacock, J, Ross, G Ashworth, A: Absence of Brca2 causes genome instability by chromosome breakage and loss associated with centrosome amplification. Curr Biol 9: 1107-1110, 1999

47. Bange, J, Zwick, E Ullrich, A: Molecular targets for breast cancer therapy and prevention. Nat Med 7: 548-552., 2001

48. Sato, N, Mizumoto, K, Nakamura, M, Maehara, N, Minamishima, YA, Nishio, S, Nagai, E Tanaka, M: Correlation between centrosome abnormalities and chromosomal instability in human pancreatic cancer cells. Cancer Genet Cytogenet 126: 13-19., 2001

49. Pihan, GA, Purohit, A, Wallace, J, Malhotra, R, Liotta, L Doxsey, SJ: Centrosome Defects Can Account for Cellular and Genetic Changes That Characterize Prostate Cancer Progression. Cancer Res 61: 2212-2219, 2001

50. Cariou, S, Donovan, JC, Flanagan, WM, Milic, A, Bhattacharya, N Slingerland, JM: Down-regulation of p21WAF1/CIP1 or p27Kip1 abrogates antiestrogen- mediated cell cycle arrest in human breast cancer cells. Proc Natl Acad Sci U S A 97: 9042-9046., 2000

51. Keyomarsi, K, Conte, D, Toyofuku, W Fox, MP: Deregulation of cyclin E in breast cancer. Oncogene 11: 941-950, 1995

Table I. Features of Breast Cancer Cell Lines and Tumor Tissue Centrosomes

Characteristics of Cell lines:

	MCF-7	T-47D	MDA-231
Centrosome Phenotype	Normal	Amplified	Amplified
Volume (μm3)	0.06	0.13	0.223
% >4 centrioles/cell	14%	38%	56%
MT Index	1.8± 0.6	2.9± 0.3	3.0 ± 0.3
Aberrant Mitosis	10%	14%	22%
Metastatic Potential	Low	Low	High
ER Status	ER+	ER+	ER-
p53	Wild-type	Mutant	Mutant

Characteristics of Breast Tumors:

Breast Tissue	Normal	Diploid Tumors	Aneuploid Tumors
Centrosome Phenotype	Normal	Normal	Amplified
Volume (μm^3)±SD	0.023 ±0.018	0.053±0.02	0.165±0.125
Number Range (Ave)	0.7-3.0 (1.29)	2.6-2.9 (2.8)	1.5-10.8 (5.6)
MT Index	1±0.05	3.7±3.4	6.6±3.1
Spindle Morphology	Bipolar	Bipolar	Aberrant
Lymph Node Positive	NA	0	6/13
ER Status	ER+	ER+	9/13 ER+
p53	Wildtype	Wildtype	8/13 Wildtype

FIGURE LEGENDS

Figure 1. Centrosome amplification in human breast tumor cell lines. Each column illustrates characteristics from the cell line indicated at the top of the figure: MCF-7, T-47D, and MDA-231. The cell lines were ordered with an increasing level of centrosome amplification from left to right. Centriole number was determined by indirect immunofluorescence for centrin (Top Row). Normal centrosomes have two or four centrioles, while amplified centrosomes have multiple centrin spots. Pericentriolar material was determined by indirect immunofluorescence for pericentrin (Second Row). Normal centrosomes show staining surrounding the two centrioles, while amplified centrosomes show excess accumulation of pericentrin (Bar = 1 μm). Microtubule nucleation (green fluorescence) in detergent extracted cells (Third Row). Nuclei were stained blue with Hoechst. Centrosome amplification results in an increased microtubule nucleating capacity. Mitotic spindle morphology was determined in cells where centrioles were stained by indirect immunofluorescence for centrin (green/yellow), and mitotic motor protein HsEg5 was stained red using antibody M4-F, and DNA was stained using Hoechst (Forth Row). Normal bipolar spindles show two centrin staining spots at each pole as illustrated for MCF-7. Increased frequency of aberrant spindle morphology is seen in tumors with amplified centrosomes (Bar = 5 μm).

Figure 2. Western blot analysis of ER, EGFR, ErbB2, p53 status, and $p21^{Waf1/Cip1}$ **expression in the three breast tumor cell lines: MCF-7, T47-D, and MDA MB 231.** Fifty micrograms of total protein was run in each lane. β-actin loading control is shown at the bottom of the figure.

Figure 3. Centrosome amplification (upper panel) and aneuploidy (lower panel) in human breast tumors. (a-e): Centrin staining in green, pericentrin staining in red and co-localization in yellow. Nuclei stained blue with Hoechst stain for DNA. (a): Normal breast tissue. (b-d): Tumor specimens are ordered with an increasing level of centrosome amplification and aneuploidy, from (b) to (d). ER, p53 and ploidy status is indicated above. The tumor shown in (b) is diploid, ER positive and p53 wild-type. The other tumors show increased aneuploidy and increased centrosome amplification (from left to

right). (a): Normal breast tissue. (b): An ER positive, p53 wild-type, lymph node negative, diploid breast tumor showing nearly normal levels of centrin and pericentrin staining. (c): ER positive, p53 mutant, lymph node negative, aneuploid breast tumor showing elevated centrin and pericentrin staining. (d): ER negative, p53 mutant, metastatic, aneuploid breast tumor showing a high level of centrin and pericentrin staining. Lower panel: Ploidy status of normal and tumor tissues. Tumors with identical ER and p53 status were also analyzed for chromosomal instability using FISH analysis for chromosomes 3 (red), 7 (green) and 17 (blue). The average values for percentage of cells showing chromosomal gains or losses are indicated. Bars = 10 μm.

Figure 4. Electron microscopy of centrosomes from normal and tumor tissues and breast cell lines. Normal centrosomes with two centrioles and nominal pericentriolar material are present in normal breast epithelial tissue (a), diploid tumors (b), the normal human mammary epithelial cell line, HMEC (e), and in MCF-7 cells (f). Examples of supernumerary centrioles are present in breast tumors (c) and MDA-MB231 cells (g), while some tumors cells also show excess pericentriolar material (d). Arrows in (g) indicate centriole profiles. Bar in d = 0.5 μm for images a-f and in g for g only.

Figure 1

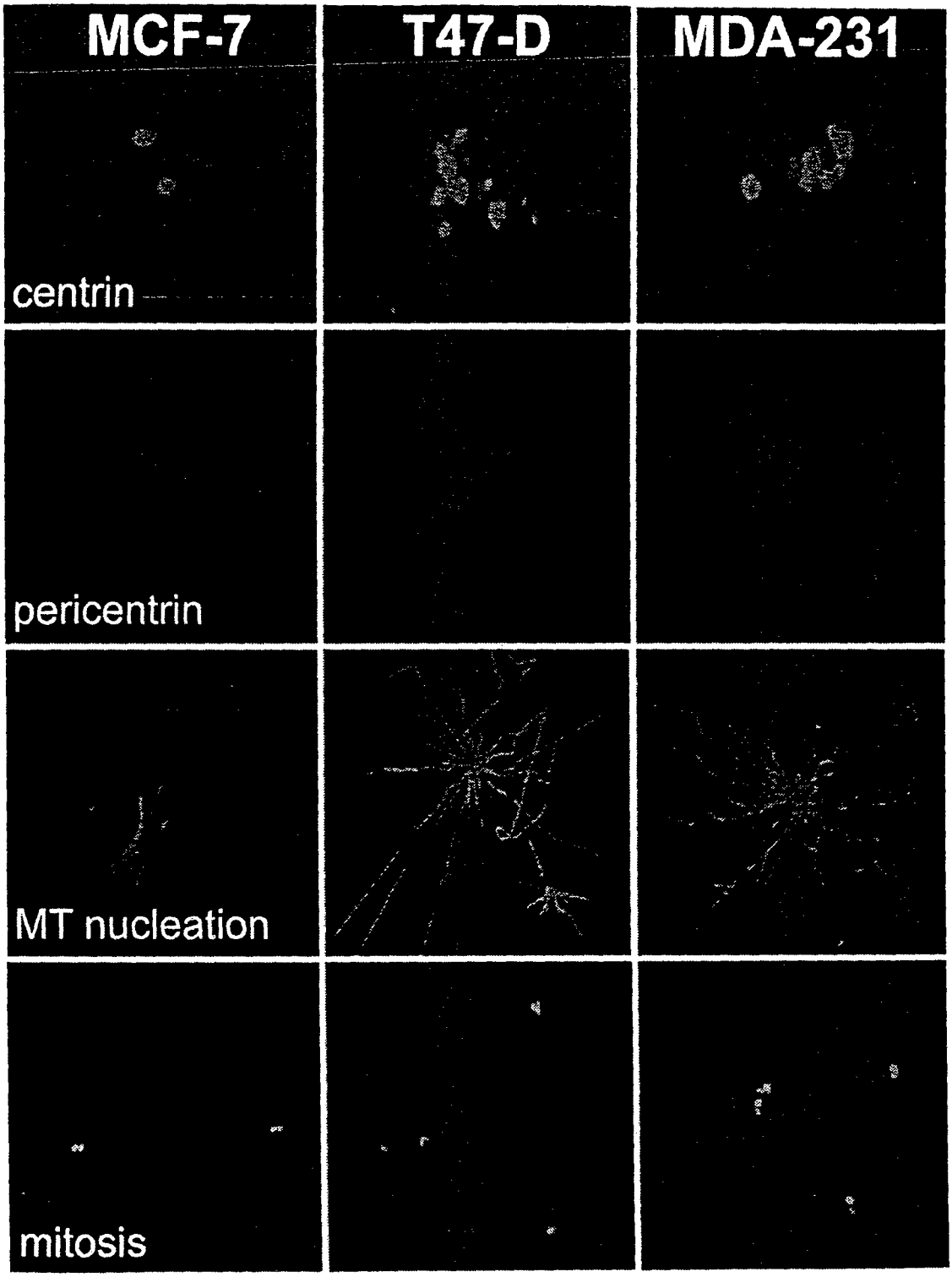
MCF-7
T47-D
MDA-231
centrin
pericentrin
MT nucleation
mitosis

Figure 2

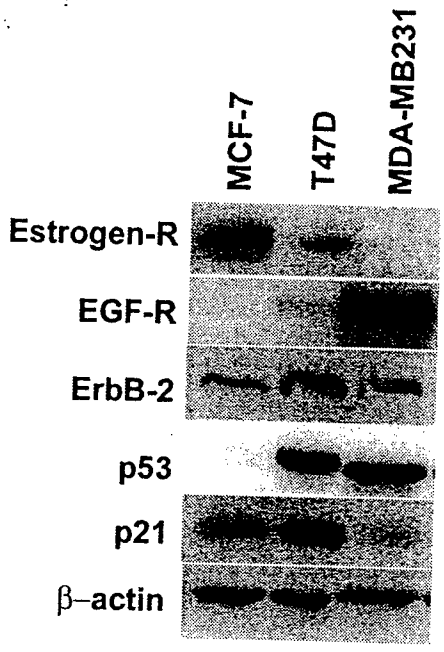

Figure 3

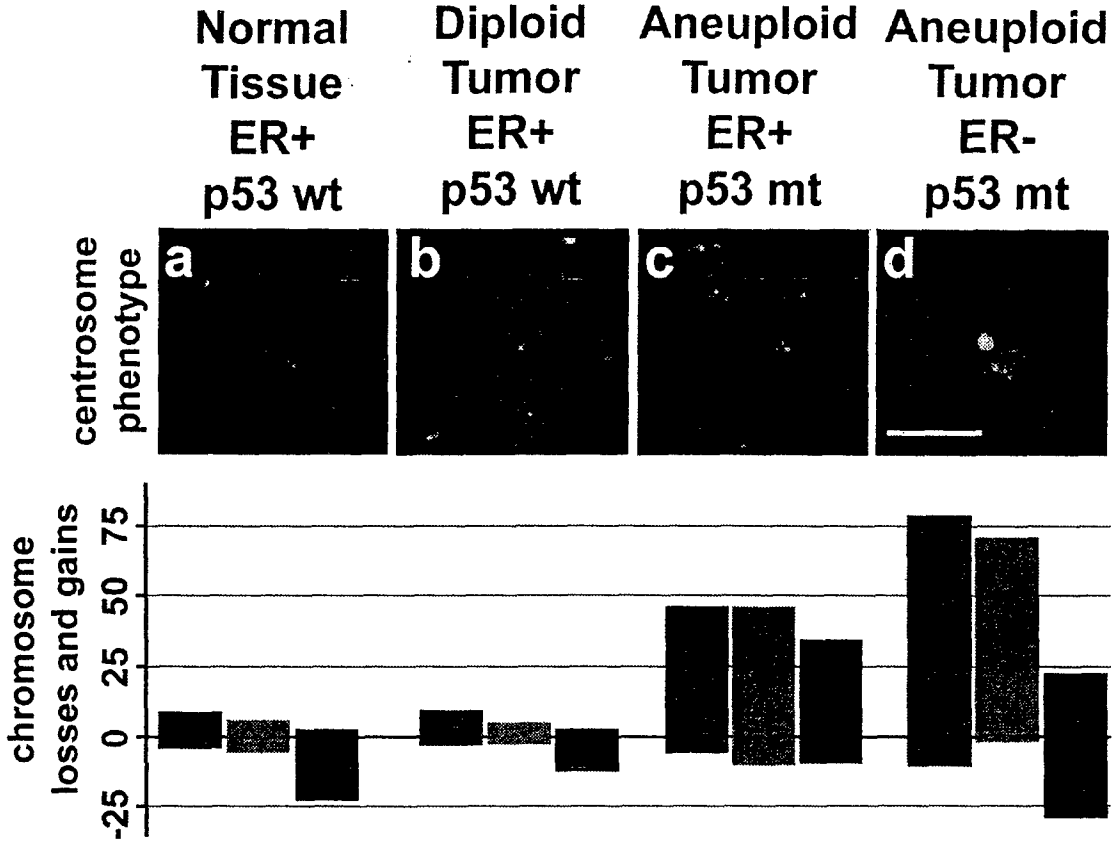
Normal Tissue ER+ p53 wt
Diploid Tumor ER+ p53 wt
Aneuploid Tumor ER+ p53 mt
Aneuploid Tumor ER- p53 mt
centrosome phenotype
a
b
c
d
chromosome losses and gains
75
50
25
0
-25

Figure 4

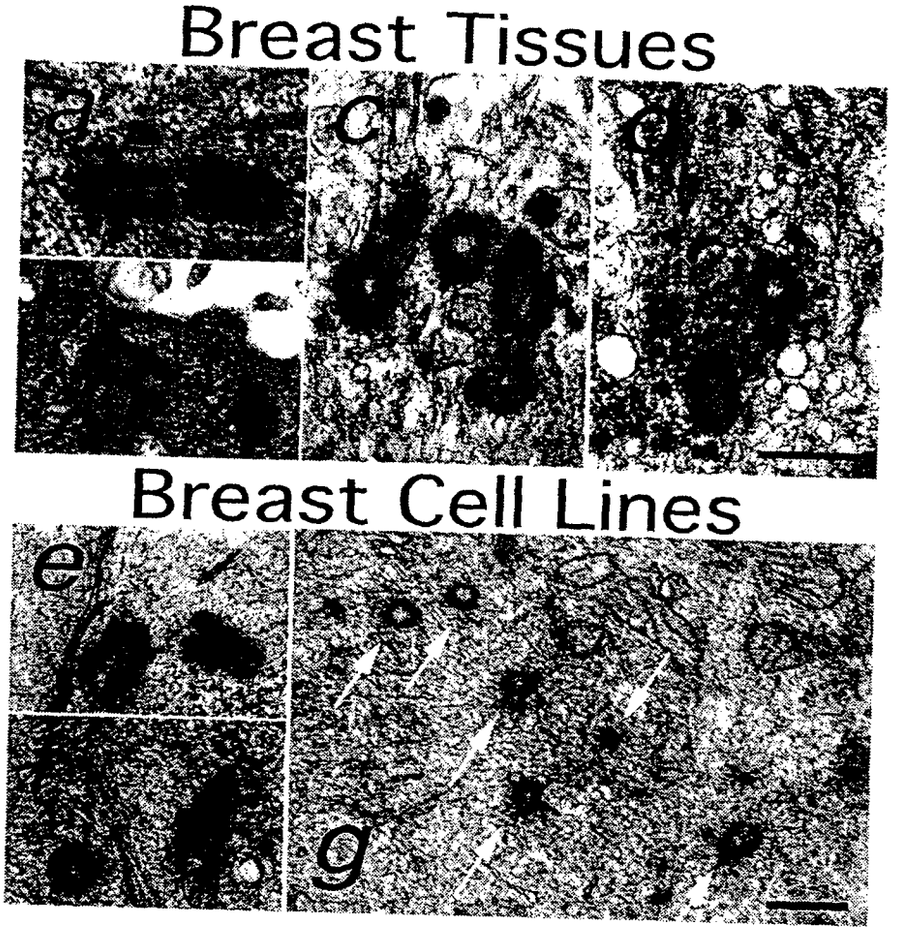

American Journal of Pathology, Vol. 155, No. 6, December 1999

Altered Centrosome Structure Is Associated with Abnormal Mitoses in Human Breast Tumors

Wilma L. Lingle and Jeffrey L. Salisbury

From the Tumor Biology Program, Mayo Foundation, Rochester, Minnesota

Centrosomes are the major microtubule organizing center in mammalian cells and establish the spindle poles during mitosis. Centrosome defects have been implicated in disease and tumor progression and have been associated with nullizygosity of the p53 tumor suppressor gene. In the present ultrastructural analysis of 31 human breast tumors, we found that centrosomes of most tumors had significant alterations compared to centrosomes of normal breast tissue. These alterations in included 1) supernumerary centrioles, 2) excess pericentriolar material, 3) disrupted centriole barrel structure, 4) unincorporated microtubule complexes, 5) centrioles of unusual length, 6) centrioles functioning as ciliary basal bodies, and 7) mispositioned centrosomes. These alterations are associated with changes in cell polarity, changes in cell and tissue differentiation, and chromosome missegregation through multipolar mitoses. Significantly, the presence of excess pericentriolar material was associated with the highest frequency of abnormal mitoses. Centrosome abnormalities may confer a mutator phenotype to tumors, occasionally yielding cells with a selective advantage that emerge and thrive, thus leading the tumor to a more aggressive state. ***(Am J Pathol 1999, 155:1941–1951)***

Checkpoints monitor the nuclear cycle and signal progression after proper completion of earlier stages of the cell cycle.[1] Differentiation, cell proliferation, and programmed cell death are normal outcomes of checkpoint surveillance. In cancer, disregulation of the cell cycle can result in either a decrease in the rate of cell death or an increase in the rate of cell division, and thereby lead to tumor growth. The orderly duplication of the centrosome once, and only once, in each cell cycle and the formation of a bipolar mitotic spindle are key cell cycle checkpoints leading to successful cell division. The importance of the centrosome in the development of malignant tumors was suspected first by Boveri[2] nearly 100 years ago. More recently, centrosome defects have been implicated in disease and tumor progression.[3–13] Defects in centrosome duplication, alteration in centrosome microtubule nucleation capacity, and inappropriate phosphorylation of centrosome proteins were first described for human breast tumors[14] and subsequently, centrosome anomalies were reported for other tumors.[15–17] Recent evidence suggests that elevated Aurora kinase or Serine/Threonime kinase-15 (STK15) activity may play a key role in acquisition of at least some of these centrosome defects during tumor progression.[18]

The centrosome is the major microtubule-organizing center in mammalian cells; it regulates the number, stability, polarity, and spatial arrangement of microtubules in interphase cells.[19,20] Thereby, the centrosome and microtubules play a role in maintaining overall cell polarity, provide an architectural framework for directed organelle transport, and participate in cell shape and movement.

The interphase centrosome consists of a pair of orthogonally oriented centrioles surrounded by a pericentriolar matrix. Duplication of the centrosome begins during S phase of the cell cycle when the two centrioles lose their orthogonal arrangement before the formation of a procentriole (or bud) closely associated with the proximal end of each of the original centrioles. The procentrioles lengthen during S and G2, so that by prophase the cell contains two diplosomes, that is, two orthogonal pairs of full-length centrioles.[21–24] At the onset of prophase, the diplosomes, along with associated pericentriolar material, move to opposite sides of the nucleus and establish the bipolar mitotic spindle.[25]

We recently have shown that the centrosomes of high-grade breast cancers do not follow this program of events.[14] In breast tumor cells, centrosome duplication is uncoupled from the cell cycle, resulting in cells with numerous centrosomes, many of which are larger than normal. Tumor centrosomes typically show inappropriate levels of phosphorylated proteins, in contrast to normal centrosomes, which contain increased levels of phosphorylated proteins during mitosis.

Here we compare the ultrastructure of centrosomes of normal breast epithelial tissues and breast adenocarcinomas. These studies reveal dramatic abnormalities in the centrioles and centrosomes of breast tumor cells. These abnormalities include 1) supernumerary centrioles, 2) excess pericentriolar material, 3) disrupted cen-

Supported by grants from the National Cancer Institute (CA72836 and CA09441) and the Department of Defense (DAMD17-98-1-8122) and by the Mayo Clinic Foundation.

Accepted for publication August 24, 1999.

Address reprint requests to Wilma L. Lingle, Tumor Biology Program, Division of Experimental Pathology, Mayo Foundation, 200 First St. S.W., Rochester, MN 55905. E-mail: lingle@mayo.edu.

triole barrel structure, 4) unincorporated microtubule complexes, 5) centrioles of unusual length, 6) centrioles functioning as ciliary basal bodies, and 7) mispositioned centrosomes. Structural centrosome abnormalities, most notably excess pericentriolar material, were associated with an increased frequency of abnormal mitoses as assessed by Ki-67-immunolabeled paraffin sections of the same tumors. The relevance of centrosome structure with regard to cell polarity, differentiation, bipolar and multipolar mitosis, and tumor progression is discussed.

Materials and Methods

Tissues

Tissues from 45 consecutive mastectomy and lumpectomy surgeries were collected according to an Institutional Review Board-approved protocol. Tissues were omitted from the analysis if patients had received previous chemotherapy or radiation therapy (n= 6), did not include primary invasive tumor (n = 4), were poorly preserved (n = 3), or were from male patients (n = 1). The remaining 31 tumors, which included two grade 2, nine grade 3, and twenty grade 4 specimens (Mayo histological grading scale), were analyzed. Six normal tissues from breast reduction surgeries were also analyzed.

Transmission Electron Microscopy Processing and Observation

Tissues were cut into small pieces and placed in fixative (4% formaldehyde, 1% glutaraldehyde in sodium phosphate buffer, pH 7.2) at 4°C for up to 36 hours. Tissues were further processed by postfixation in osmium tetroxide, *en bloc* staining with uranyl acetate, dehydration in ethanol, and embedding in epoxy resin. Thin sections were poststained with lead citrate and examined using a Philips CM10 Biotwin transmission electron microscope (Philips Electronic Instruments, Mahwah, NJ). Tissues were categorized according to centrosome location, number of centrioles in thin section, qualitative level of pericentriolar material, presence and arrangement of centriolar appendages, presence of primary cilia, variations on centriolar structure, and multipolar mitotic figures.

Light Microscopy and Mitotic Index Determination

Portions of tissues also were formalin-fixed and paraffin-embedded for light microscopy. Sections were immunostained using MIB-1 antibody against Ki-67 (Dako Corp., Carpinteria, CA). Ki-67 is a nuclear antigen that is present in late G1, S, G2, and mitotic cells, but is lacking in G0 and early G1 cells. Condensed chromosomes are stained intensely with this antibody, allowing for easy quantification of proliferative and mitotic cells and identification of abnormal mitotic figures. Proliferative index (PI) was calculated as the percentage of Ki67-positive cells out of the total number of epithelial cells. A minimum of 200 cells was counted in defined fields of view using a 40× objective. Likewise, mitotic index (MI) was calculated as the percentage of mitotic cells in the same fields of view. When no mitotic cells were observed, the MI was calculated as <1 mitotic cell per the total number of cells observed. Because the frequency of abnormal mitotic figures is very low in most tissues, the abnormal mitotic index (AMI) was determined by scanning the entire section and counting the total number of mitotic cells and the total number of abnormal mitotic figures. The ratio of abnormal to total mitoses was then multiplied by the mitotic index to yield the AMI. These data are summarized in Figure 7. All tissues were scored blindly. Photographs were made using a Nikon FXA photomicroscope.

Centrin Immunofluorescence

A subset of tissues was selected for immunofluorescence studies. These tissues included one tumor with normal centrosome ultrastructure, one tumor with clusters of extra centrioles, two tumors with extra pericentriolar material, and two tumors with inverted polarity. Normal tissue used for immunofluorescence was from a different patient than that used in the ultrastructure studies. All tissues were frozen in liquid nitrogen within 30 minutes of surgical removal and stored at −70°C until use. Cryosections were immunostained with a monoclonal antibody against centrin, a centrosomal protein, as previously described.[14] Sections were examined and photographed using a Nikon FXA epifluorescence microscope.

Results

Normal Breast Epithelium

Normal breast epithelial tissues were organized with a high cuboidal layer of luminal cells separated at intervals from the basement membrane by a discontinuous layer of myoepithelial cells (Figure 1, A and B). The nuclei of the luminal epithelial cells tended to be basal and the centrioles apical. Although apical, most often the position of the centrioles was eccentric; that is, they were located near the lateral junctional complexes of adjacent cells (Figure 1B). Although centrioles usually did not maintain an orthogonal orientation, they were typically close to each other (Figure 1, A and C). Occasionally, an extremely short primary cilium extended from the distal end of the mature centriole (Figure 1C). Fine striated rootlets infrequently were observed extending from the proximal ends of centrioles toward the base of the cell (Figure 1D). The striated rootlets were quite variable in extent and were not observed with most centrioles. Other than distal and subdistal appendages on the mature centriole and fine fibrillar material along the outer walls of the centriole barrels, little pericentriolar material was noted with the centrioles of normal luminal epithelial cells (Figure 1, A-D). Subdistal appendages were slightly more developed on the centrioles of the myoepithelial cells, and their primary cilia were longer than those of luminal epithelial

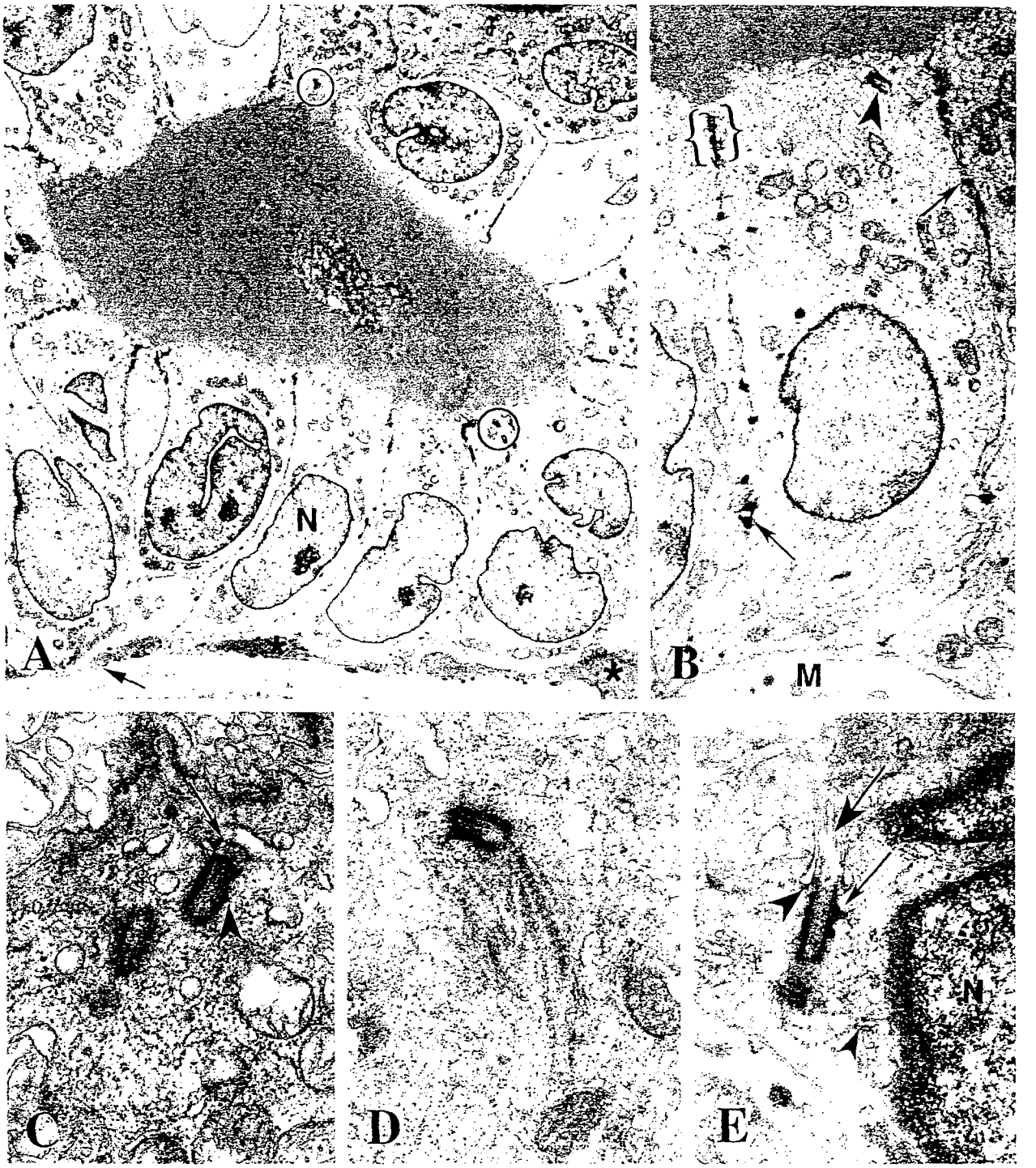

Figure 1. Normal breast epithelium. **A:** The normal breast ductal epithelium consists of a high cuboidal layer of luminal cells subtended by a discontinuous layer of myoepithelial cells (*) and basement membrane (**arrow**). The nuclei (N) are basal and the centrosomes (**circled**) are apical. **B:** Adjacent luminal epithelial cells are joined by lateral junctional complexes (**brackets**) near the apical membrane and desmosomes (**arrows**) between their lateral membranes. A single centriole (**arrowhead**) is located at the apex next to a junctional complex. A portion of a myoepithelial cell (M) is seen at the base of the luminal epithelial cell. **C:** The mature centriole of this nonorthogonal diplosome bears a short primary cilium (**arrow**) at its distal end in this luminal epithelial cell. A small subdistal appendage (**arrowhead**) is present on the mature centriole, whereas the immature centriole lacks appendages. Although very little pericentriolar material is present, the centrioles do have a coating of fine fibers. **D:** A striated rootlet extends from the proximal end of this mature centriole toward the base of the luminal epithelial cell. **E:** Fine fibers (**small arrowhead**) extend between the diplosome and the nearby nucleus (N) in this myoepithelial cell. Distal appendages (**large arrowhead**) extend between the centriole and the plasma membrane at the site of primary cilium (**large arrow**) emergence. Subdistal appendages (**small arrow**) are prominent on the mature centriole. The immature centriole is seen in oblique section. Original magnifications, ×3500 (**A**), ×8850 (**B**), ×27,500 (**C**), ×25,600 (**D**), ×21,200 (**E**).

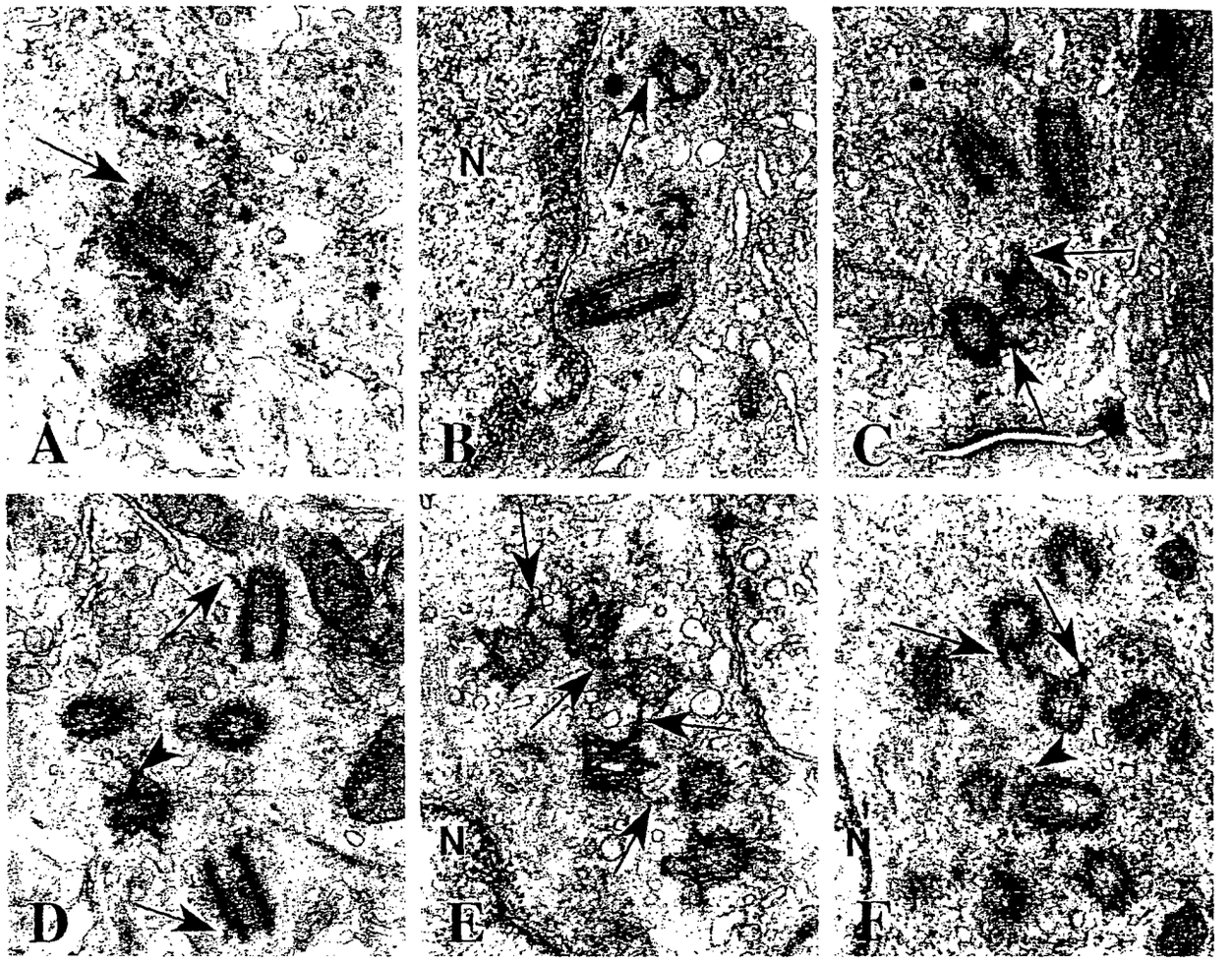

Figure 2. Supernumerary centrioles in breast tumors. **A:** A procentriole (**arrow**) is present at the proximal end of one of the two centrioles in this section. This procentriole is identifiable by its orthogonal orientation relative to the full length centriole and by the width of its lumen. Notice the electron opaque pericentriolar satellites surrounding the centrioles. **B:** Two centrioles are seen in cross section and a third is in longitudinal section. One centriole has subdistal appendages (**arrow**). All three are close to the nucleus (N). There is no orthogonal relationship between any of the three centrioles. **C:** At least two of these four centrioles have subdistal appendages (**arrows**). **D:** The barrels of these five centrioles are coated with a fine electron opaque material. Two centrioles have distal appendages (**arrows**) and at least one also has subdistal appendages (**arrowhead**). **E:** This group of six centrioles is linked by fine fibers between their subdistal appendages (**arrows**). The group is next to the nucleus (N). **F:** At least nine centriole profiles are present in this thin section. Subdistal (**arrows**) and distal (**arrowhead**) appendages are seen on many of the centrioles. The nucleus (N) is adjacent to this cluster of centrioles. Original magnifications, ×27,500 (**A** and **B**), ×32,300 (**C** and **F**), ×31,000 (**D**), ×34,150 (**E**).

cells (Figure 1, B and E). Unlike luminal epithelial cells, diplosomes of myoepithelial cells were located close to the nuclei. Filaments extended from the myoepithelial diplosome to the nucleus (Figure 1E); this was never observed in luminal epithelial cells. No centrosome abnormalities were observed in normal epithelial cells of the four reduction mammoplasties examined by electron microscopy.

Invasive Breast Tumors

Twenty-four of 31 invasive tumors contained centrosomes and that differed from those of normal breast cells in a variety of ways. Eleven tumors were characterized by centrosomes with more than two centrioles (Figures 2 and 3, A-C). In thin sections, these supernumerary centrioles ranged from a pair of centrioles with a single extra procentriole to a field of 9 centriole profiles (Figure 2, A-F). Often the extra centrioles were arranged in a group and were closely linked by fine fibers extending between subdistal appendages (Figure 2, C, E, and F). Appendages normally associated with only the mature centriole were seen frequently with more than one centriole in these groups (Figure 2, C-F, and Figure 3A). Centrosomes with extra centrioles were most often located adjacent to the nucleus (Figure 2, B, E, and F), in contrast to normal luminal epithelial cells, in which the centrioles tended to be closer to the apical plasma membrane (Figure 1, A and B).

The amount of pericentriolar material and satellites associated with tumor centrosomes was variable, ranging from low levels similar to normal centrosomes (Figure 2, B-F), to moderate (Figure 2A) and excessive levels (Figure 3). In all, nine tumors had excess pericentriolar material, often in addition to extra centrioles. In some tumors this pericentriolar material had a distinct fibrogranular appearance (Figures 2A and 3) reminiscent of material associated with basal body formation in ciliated

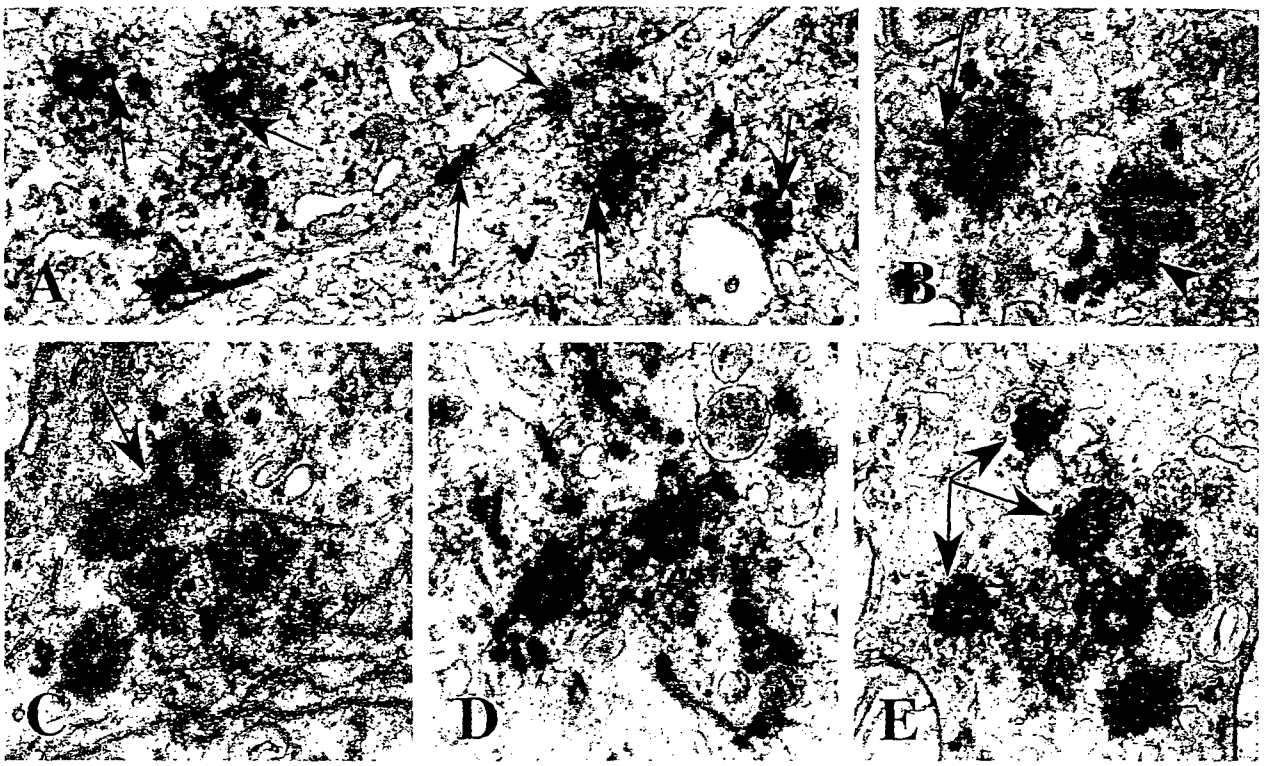

Figure 3. Excess pericentriolar material in breast tumors. **A:** Centrosomes in two adjacent cells are seen. Desmosomes (**small arrows**) tether the plasma membranes. All of the centriole profiles include subdistal appendages that are characteristic of mature centrioles (**large arrows**). Electron opaque fibrogranular material is present around both centrosomes. **B:** The barrels of these centrioles are coated with a dark granular material and pericentriolar satellites are present. One centriole has distal and subdistal appendages (**arrow**) while the other has a procentriole (**arrowhead**) associated with it. **C:** Fine electron opaque fibers coat the five centriole profiles seen in this section. Two orthogonal centrioles are connected by a dense parallel array of fibers (**arrow**). **D:** Two centrioles with numerous dark granules are present in this section. **E:** This centrosome contains one centriole and several masses (**arrows**) similar to generative complexes visible in this section. Original magnifications, ×17,900 (**A**), ×31,650 (**B**), ×28,000 (**C**), ×28,700 (**D**), ×27,650 (**E**).

cells. Large granular masses, similar to generative complexes involved in ciliary basal body formation, were also observed in the pericentriolar material in some tumor cells (Figure 3E). Many centrioles were encased in electron opaque material pressed directly to the barrel of the centriole (Figure 3, B and C).

In addition to excessive pericentriolar material, two tumors had centrioles that were structurally defective in various aspects (Figure 4). Normal centrioles are composed of nine sets of triplet microtubules in which the A microtubule is complete and the B and C microtubules share protofilaments with A and B, respectively.[26] Unusual microtubule complexes were observed near complete centrioles in some tumors (Figure 4A). These microtubule complexes were not assembled into normal triplets nor arranged in a barrel shape; rather they were an assortment that included five or more microtubules with shared protofilaments embedded in amorphous electron-opaque material (Figure 4A). In one instance a centriolar microtubule triplet was displaced away from the centriole barrel, resulting in what has been termed an open ring centriole (Figure 4B). Unusually long centrioles (Figure 4D) were observed in one tumor. Primary cilia ranged from very short to well developed (Figure 4C).

Some tumors had regions of apocrine metaplasia in which luminal epithelial cells maintained normal apical/basal polarity, but had cytoplasmic beaks that projected into the lumen (Figure 5A). The beaks were bordered by the apical plasma membrane that protruded well past the junctional complexes that mark the apical limit of the lateral plasma membrane. Beak cytoplasm contained numerous secretory vesicles, endoplasmic reticulum, and mitochondria. The centrosomes in these cells were near the junctional complexes and just apical to the nucleus, but not adjacent to the lumen as in normal luminal epithelial cells (Figure 5A). In one well differentiated grade 2 tumor with apocrine metaplasia, the beaked apocrine cells were mixed with ciliated cells. The ciliated cells also maintained apical/basal polarity, but along their apical membrane were numerous cilia with centrioles functioning as ciliary basal bodies (Figure 5B). These cilia and basal bodies were similar in location and appearance to those of normally ciliated cells such as ciliated respiratory epithelium. Microvilli also were located along the apical membranes of the ciliated cells (Figure 5B). The apical membranes of the ciliated cells did not protrude into the lumen as did the nonciliated beaked cells (Figure 5A). Both the ciliated and the beaked cells were in regions of tumors that were well differentiated.

Two tumors contained regions in which cells still maintained apical/basal polarity even in poorly differentiated and highly invasive tumors lacking a basement membrane (Figure 5C). The apical and lateral membranes were identified by their location relative to junctional complexes and the presence of microvilli on the apical membrane. In these instances, the cell apices often did not

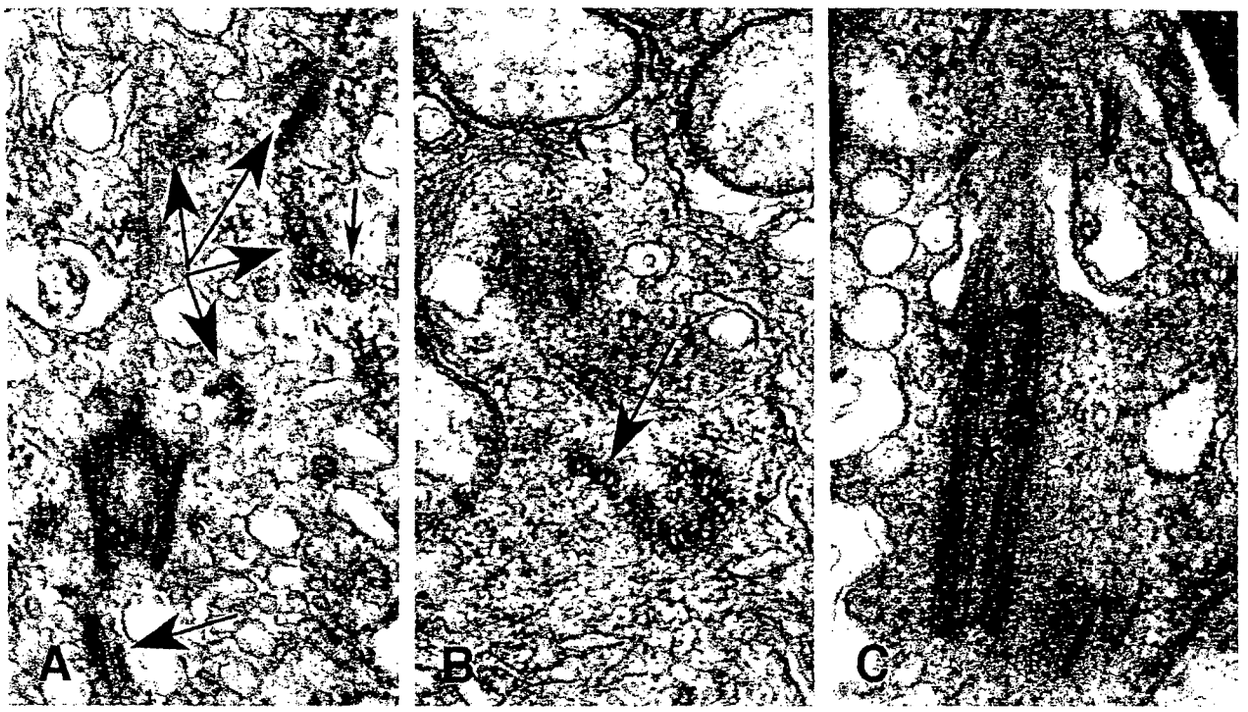

Figure 4. Abnormal centriole structure in breast tumors. **A:** Subdistal appendages are seen in this oblique section through a centriole. Numerous microtubule complexes (**large arrows**) are seen in various planes of section throughout the cytoplasm near the centriole. As is seen in cross section of the complexes, the individual microtubules share a portion of the wall of the neighbor microtubules (**small arrow**). **B:** The open-ring configuration of this centriole is shown in cross section. Two of the nine triplet microtubule complexes are splayed away from the centriole barrel (**arrow**). **C:** This centriole bearing a primary cilium (*) is nearly twice as long as normal centrioles. Original magnifications, ×54,500 (**A**), ×59,625 (**B**), ×47,700 (**C**).

face a lumen, but instead faced collagen fibrils of the stromal connective tissue (Figure 5C). The centrosomes of these cells were normal in structure and were located next to the junctional complexes near the apical plasma membrane, but, because the apices face the stroma, the cell polarity was inverted.

Mitosis in Tumor Cells

Although mitotic figures were not observed in normal breast tissues, there were numerous mitotic figures present in four of the tumors examined transmission electron microscopy. Some mitotic figures appeared normal in thin section, having a typical metaphase plate and bipolar spindle (not shown), whereas others had significant abnormalities (Figure 6). A tripolar mitosis is shown in Figure 6A. Tracings of microtubules, spindle poles, and condensed chromosomes from six nonadjacent serial sections through the cell in Figure 6A are presented in Figure 6B. Analysis of the reconstruction in three dimensions revealed that one spindle pole was composed of two distinct but adjacent foci of microtubules, which perhaps resulted from their coalescence in prometaphase. Each spindle pole had at least two centrioles recognizable as distinct structures in these six nonadjacent thin sections. Many division figures were too bizarre for analysis in thin section.

Centrin Immunofluorescence

As previously described,[14] normal breast tissues have an apically positioned pair of immunolabeled spots that correspond to the centrioles (Figure 6E). Pairs of spots also were observed in cells of the tumor with normal centrosome ultrastructure, although the tissue was anaplastic and centriole location appeared random (Figure 6F). Many cells in the tumor with numerous centrioles closely linked by fine fibers contained clusters of spots the size and shape of centrioles (Figure 6G), whereas spots of various sizes and shapes were present in cells of the tumors characterized by extra pericentriolar material (Figure 6H).

Proliferation and Mitotic Indices

Indices of proliferation, mitosis, and abnormal mitosis are summarized in Figure 7. Tissues were placed in one of four categories on the basis of tissue type and centriole/centrosome structure. Category I is comprised of all normal tissues from reduction mammoplasty. All six of these tissues had normal centrosome structure as assessed by immunofluorescence and/or electron microscopy. Category II consists of the nine tumors that have normal centriole/centrosome structure as assessed by immunofluorescence and electron microscopy. Category III contains twelve tumors with abnormal centriole/centrosome structure such as supernumerary centrioles or structur-

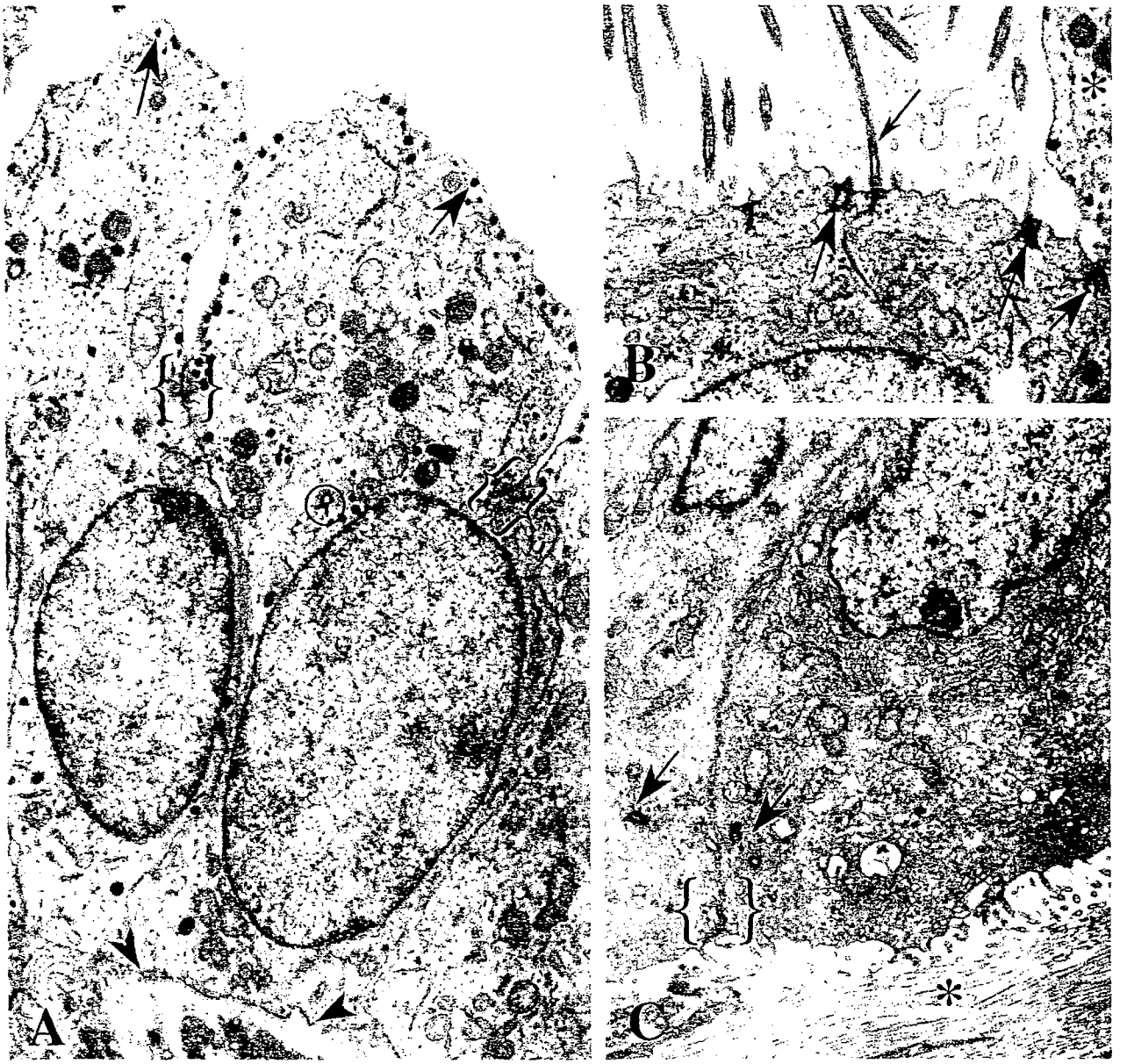

Figure 5. Positional centrosomal anomalies in breast tumors. **A:** Secretory granules (**arrows**) are present at the apical membrane of these cells displaying apocrine metaplasia. Junctional complexes (**brackets**) mark the transition from lateral to apical membrane domains. Apocrine beaks extend into the lumen of the duct. Notice the centriole (**circled**) near the apical end of the nucleus. These cells have apical/basal polarity and rest on a basement membrane (**arrowheads**). **B:** Extra centrioles in this cell are inserted at the apical plasma membrane where they function as basal bodies (**large arrows**) for cilia (**small arrow**). Microvilli and cilia project into the lumen. The beak of an adjacent apocrine cell (*) is visible. The ciliated cell does not protrude into the lumen, as does the apocrine cell; but like its apocrine neighbor, it has apical/basal polarity and rests on a basement membrane (not visible in this figure). **C:** The two centrosomes (**arrows**) seen in adjacent cells are located near the junctional complex between these polarized cells (**bracket**). However the apical membrane domain with microvilli faces collagen (*) of the stromal tissue rather than the lumen of a duct. This invasive group of cells has ramified through the breast stroma and is not subtended by a basement membrane. The polarity of these cells is inverted, with the basal domains abutting the basal domains of other cells and the apical domains facing the stroma rather than a lumen. Original magnifications, ×8150 (**A**), ×10,000 (**B**), ×7900 (**C**).

ally defective centrioles. Tumors with excess pericentriolar material in addition to centriole abnormalities are excluded from this category and placed in Category IV. Category IV contains seven tumors with excess pericentriolar material, regardless of other centriole/centrosome characteristics.

The six normal breast tissues (Category I, Figure 7) examined by light microscopy had a median PI of 5.3% as determined by Ki67 immunostaining. These normal tissues had a median MI of 0.00% (mean mitotic index = 0.03%) based on the total of 4238 epithelial cells observed. On examination of entire histological sections from all six tissues, only two contained identifiable mitotic figures, and no abnormal mitotic figures were observed. Of the nine tumors with normal centriole/centrosome ultrastructure (Category II, Figure 7), five contained no abnormal mitotic figures and four did, yielding a median AMI of 0.00% (mean = 0.16%). The median PI, MI, and AMI of Category II tumors were not significantly different from Category III tumors.

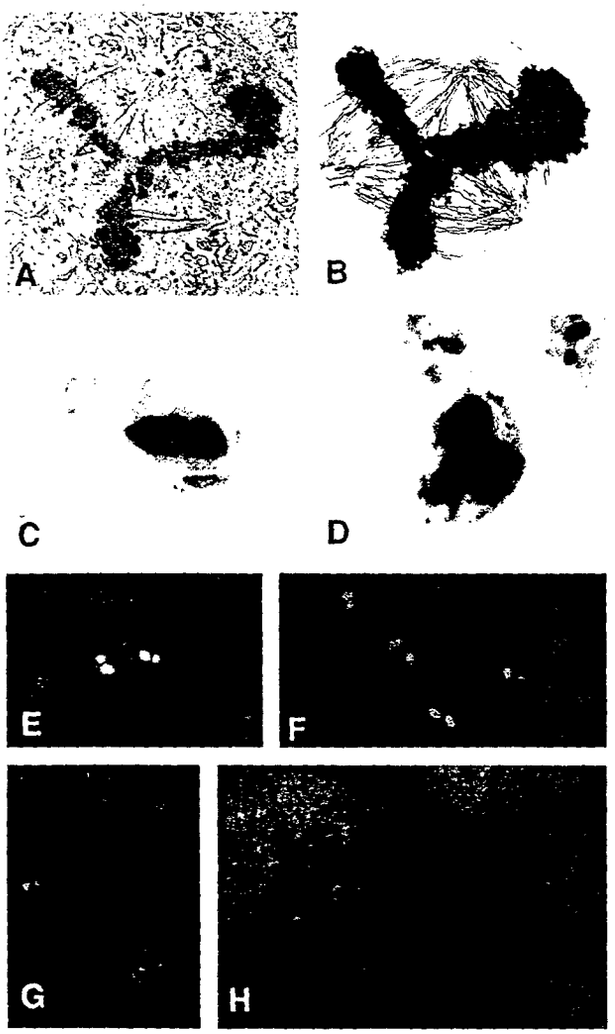

Figure 6. Multipolar mitoses and centrin immunofluorescence. **A:** This section through a symmetrical tripolar mitotic cell shows part of the metaphase plate and portions of the tripolar spindle. **B:** Tracings of microtubules (red), spindle poles (green), and condensed chromosomes (blue) from six nonadjacent serial sections through the cell shown in **A** are shown in this overlay. The upper spindle pole appears to contain two separate, but adjacent, microtubule foci that have coalesced. **C:** A normal metaphase plate is shown in this Ki-67 immunostained paraffin section of a breast tumor. **D:** A tripolar metaphase cell immunolabeled with Ki-67 is shown in this tumor section. **E:** In normal breast epithelium, the centrosomes appear as distinct pairs of spots when labeled with antibodies against centrin. Centrosomes of two adjacent cells are shown in this cryosection. **F:** In this tumor characterized with normal centrosome ultrastructure, the centrosomes are similar to those of normal tissue when immunolabeled using antibodies against centrin. **G:** Centrin immunofluorescence of the same tumor shown in Figure 2, E and F, reveals a cluster of centriole-sized spots as well as a normal looking pair of spots. By transmission electron microscopy this tumor had up to 9 centrioles in a single thin section, but no excess pericentriolar material. **H:** Centrin immunofluorescence of the same tumor as shown in Figures 3D and 6A reveals numerous large, amorphous spots. By transmission electron microscopy, centrosomes of this tumor contain excess pericentriolar material and extra centrioles. Original magnifications, ×160 (**A** and **B**), × 925 (**C** and **D**), ×2050 (**E-H**).

The Category IV tumors, characterized by the presence of excess pericentriolar material, had the highest median frequencies of proliferation, mitosis, and abnormal mitosis (28.2%, 0.71%, and 0.46%, respectively). Category IV values, with the exception of the PI relative to Category III, were significantly different from the values of all other categories.

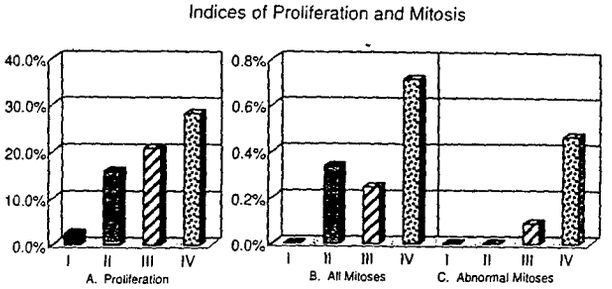

Figure 7. Indices of proliferation and mitosis. Tissues were placed in categories as follows: I (**solid black bars**), six normal tissues from reduction mammoplasties with normal centriole/centrosome structure (all normal tissues examined fell in this category); II (**solid gray bars**), nine tumor tissues with normal centrioles/centrosomes; III (**striped bars**), twelve tumor tissues with abnormal centrioles (this includes tissues with supernumerary centrioles and those with centriole defects, but excludes those with excess pericentriolar material); and IV (**stippled bars**), seven tumor tissues with excess pericentriolar material, regardless of centriole defects. The Wilcoxon Rank Sum Test was used to determine statistical significance. Median values are plotted. **A:** The proliferation index of category I (normal tissue) is significantly lower than the other three categories and that of category IV (tumors with excess pericentriolar material) is significantly greater than categories I and II, but not III. Categories II and III are not significantly different from each other. **B** and **C:** Category IV has significantly higher frequencies of mitosis and abnormal mitosis than the other three categories. The other categories were not significantly different from each other.

Discussion

The centrosome functions to nucleate and organize microtubules; during interphase the centrosome is the primary microtubule organizing center, and during mitosis duplicated centrosomes serve as mitotic spindle poles.[19] We found that centrosomes in normal breast tissue are apical and usually adjacent to the junctional complex, whereas nuclei are basal. Very little pericentriolar material is associated with these centrosomes. As is seen in other polarized epithelial cells,[27] centrioles may separate a short distance from each other after losing their orthogonal orientation, and the mature centriole may form a short primary cilium. In addition, centrioles occasionally bear a striated rootlet.

Only by selecting breast biopsy tissue from premenopausal women in the luteal phase of the menstrual cycle was Ferguson[28] able to investigate mitosis in normal breast parenchyma. In these normal cells, very little pericentriolar material was associated with the spindle poles. The normal tissues in the present study were not selected according to the phase of menstrual cycle, and no mitoses were observed by transmission electron microscopy or by light microscopy. However, normal breast epithelium does maintain a population of proliferating cells that immunostain with antibodies to Ki67; our median PI value of 5.3% in normal breast epithelium is within the range of published values.[29] In agreement with our observations on interphase cells by immunofluorescence and by transmission electron microscopy, Ferguson[28] noted that centrioles of normal interphase cells were apical and not associated with the basal nuclei. Likewise, primary cilia have previously been noted in myoepithelial cells.[30]

Centrosomes undergo changes throughout the cell cycle.[21–24] The nuclear and centrosome cycles are synchronized by checkpoints that prevent DNA reduplication before karyokinesis and prevent centrosome reduplica-

tion before anaphase. In certain normal cell types such as binuclear mouse hepatocytes[31] and human megakaryocytes,[32] synchrony between the nuclear and centrosome cycles is maintained even in the absence of cytokinesis, resulting in polyploid cells with centrosome numbers appropriate for the level of ploidy. Due to the numerous centrosomes arranged around the polyploid nucleus, megakaryocytes lack apical/basal polarity, although they do have a radial organization. In contrast, cancer cells have asynchronous nuclear and centrosome cycles, often resulting in multicentrosomal aneuploid cells that lack apical/basal polarity and appear disorganized.

We have shown that centrosomes and centrioles of most human breast tumors (24 of 31 analyzed) display a range of significant structural and functional abnormalities. Breast tissues can be divided into four categories: normal tissue with structurally normal centriole/centrosomes (Category I), tumors with structurally normal centriole/centrosomes (Category II), tumors with centriole-based abnormalities (Category III), and tumors with excess pericentriolar material (Category IV). Category IV tumors are associated with significantly increased frequencies of both normal and abnormal mitoses. Cells having no visible centrosome abnormality are also present in all tumors. Some abnormalities may be related to loss of synchrony between the centrosome cycle and nuclear cycle.

Tumor cells that become ciliated retain apical/basal polarity and tend to be well differentiated. These tumors are included in Category III. Ciliated cells have been described infrequently in breast carcinomas.[33] These multiple centrioles probably arise through the same acentriolar basal body neogenesis that occurs in normal ciliated epithelial cells.[34–37] In effect, these cells differentiate into the wrong cell type, resulting in metaplasia rather than anaplasia. These ciliated breast tumors have PI and MI of 20% and 0.2%, respectively, similar to normal breast epithelium. The ciliated cells, like normal ciliated epithelial cells, probably are terminally differentiated and remain in G0 of the cell cycle. Therefore, the production of centrioles that function as ciliary basal bodies may be a relatively harmless structural alteration with no adverse implications for genetic stability.

Open-ring centrioles and centrioles missing triplet microtubles (MTs) occur in some Category III tumors. Although these structures are similar to those present during basal body formation in hamster ciliogenesis,[38] no cilia are present in these tumors. Disrupted centriole barrels similar to open-ring centrioles have also been observed as a consequence of infection with and treatment with DNA-binding dyes,[39] and DNA-binding dyes have been shown to induce multipolar mitoses in cultured cells.[39] However, in the present study, open ring centrioles are not associated with an increase in the frequency of multipolar mitoses.

Unusual microtubule complexes embedded in dark amorphous material were also noted in one Category III tumor. The PI, MI, and AMI of this tumor are not significantly different from those of tumors with normal centrosome structure. These novel structures have not been described previously, and their importance is not understood. They may be a further indication that the mechanics, as well as timing, of centriole formation is not well regulated in tumors.

Some tumors (11 of 31 studied) produce extra centrioles that do not serve as ciliary basal bodies. In some cells of these Category III tumors, centrioles often appear linked closely together by fine fibers and remain near the nucleus. These tumors are anaplastic; ie, they are not as differentiated as tumors that produce cilia and do not retain apical/basal cell polarity. The presence of procentrioles along the proximal walls of mature centrioles indicates that these extra centrioles arose through template driven duplication rather than through acentriolar neogenesis typical of basal body production in ciliated cells.[35] Fine fibers linking the centrioles in tumors are similar to those described linking the pair of centrioles of a diplosome,[40] further supporting the idea that they originate as procentrioles associated with a mature centriole. Because template-driven centriole duplication normally occurs only once per nuclear cycle, these cells have lost the synchrony between the nuclear cycle and the centrosome cycle. As long as the centrioles remain linked together, they may function as one large centrosome in an interphase cell. However, if these large centrosomes separate into more than two spindle poles at the onset of mitosis, it is likely that chromosomal missegregation will occur, resulting in aneuploidy. Indeed, the frequency of abnormal mitoses is quite variable among these tumors, indicating that most cells with extra centrioles are capable of forming bipolar spindles.

Other tumors (9 of 31 studied, 7 of which were available for proliferation and mitotic index determination) accumulate excess pericentriolar material with their centrosomes and variable numbers of extra centrioles (Category IV tumors). The nature of the pericentriolar material is reminiscent of fibrogranular material and generative complexes associated with acentriolar as well as centriolar basal body formation.[34–37,41] However, no cilia are observed and the randomly positioned centrioles are not located near the plasma membrane. This accumulation of excess pericentriolar material may be the result of overexpression of centrosomal proteins or the reorganization of material that is normally dispersed within the cytoplasm.[14,42,43] Increased levels of γ-tubulin,[14,17] pericentrin,[15] and centrin[14] have been demonstrated in abnormal centrosomes in human tumors, and it is likely that other centrosomal proteins are present in increased levels as well. γ-tubulin-containing complexes located in the pericentriolar material are the site of microtubule nucleation, and as such are key to centrosome function.[44] We have shown that tumors with excess pericentriolar material are highly anaplastic and have lost cell polarity. These Category IV tumors tend to have higher median frequency of abnormal mitoses (0.46%) compared to tumors with other centrosome abnormalities (0.09%). This higher frequency of abnormal mitoses in tumors with extra pericentriolar material suggests that the regulation of accumulation of centrosomal proteins is more critical than regulation of centriole duplication for proper centrosome function during the cell cycle.

Some cells have more than two centrosomes that can function as spindle poles, yielding atypical multipolar mitoses. Atypical mitoses have been observed in breast tumors and other pathological specimens such as ulcerative colitis[7] and a mouse model of pancreatic cancer.[3] Multipolar mitoses were observed in several breast tumors in the present study. Aberrant mitoses such as these may arrest in metaphase, with the cells eventually undergoing apoptosis. In some instances, however, a selective advantage may be conferred to one of the daughter cells, leading to a clone of cells with chromosome gains and/or losses.

Serial sectioning through mitotic tumor cells showed that spindle poles are sometimes composed of more than one focus of microtubules. These spindle poles likely resulted from the coalescence of two or more centrosomes before metaphase. Coalescence of centrosomes could allow the formation of a bipolar spindle in a cell having extra centrosomes. Coalescence of extra centrosomes may be a mechanism by which cells can minimize the rate at which aneuploidy develops in tumors. Because compounded aneuploidy ultimately would be a self-limiting characteristic of tumors, a proportion of bipolar mitoses must be maintained for tumor growth.

The centrosomal abnormalities described here in breast tumor cells reflect changes in the status of cell and tissue differentiation of the tumors. Differentiated tumors have centrosomes of more normal appearance that are either mislocated, as in the tumors with inverted cell polarity, or perform a normal function not typical of mammary epithelial cells, such as producing ciliary basal bodies in tumors displaying apocrine metaplasia. Centrosome abnormalities are characteristic of poorly differentiated anaplastic tumors that have lost checkpoint synchronization of nuclear and centrosome cycles. This loss is reflected in centrosome defects and multipolar mitoses. As recognized by Boveri[2] earlier in this century, defective centrosomes may decrease the fidelity of chromosome segregation during multipolar mitoses. Consequently, centrosome abnormalities such as those described here may confer a mutator phenotype to tumor cells. As is the case for the molecular mutator phenotype, most mutated progeny will not be viable, but occasionally progeny with a selective advantage will emerge and thrive, and thus the tumor progresses to a more aggressive state.

Acknowledgments

We thank Ms. Denise Morgan and Ms. Belinda Hoebing of the Surgical Pathology Laboratory and the staff of the Electron Microscopy Core Facility for collecting and processing tissues used in this study and Ms. Linda Murphy for preparation of the Ki-67-immunostained slides. Dr. Vera Suman, Cancer Center Statistics, analyzed the proliferation and mitosis data.

References

1. Hartwell LH, Weinert TA: Checkpoints: controls that ensure the order of cell cycle events. Science 1989, 246:629–634
2. Boveri T: Zur Frage der Emtstehung Maligner Tumoren. Fischer Verlag, Jena, 1914. English translation by Boveri M, The Origin of Malignant Tumors. Baltimore, Waverly Press, 1929
3. Levine DS, Sanchez CA, Rabinovitch PS, Reid BJ: Formation of the tetraploid intermediate is associated with the development of cells with more than four centrioles in the elastase-simian virus 40 tumor antigen transgenic mouse model of pancreatic cancer. Proc Natl Acad Sci USA 1991, 88:6427–6431
4. Balczon R, Bao L, Zimmer WE, Brown K, Zinkowski RP, Brinkley BR: Dissociation of centrosome replication events from cycles of DNA synthesis and mitotic division in hydroxyurea-arrested Chinese hamster ovary cells. J Cell Biol 1995, 130:105–115
5. Cross SM, Sanchez CA, Morgan CA, Schimke MK, Ramel S, Idzerda RL, Raskind WH, Reid BJ: A p53-dependent mouse spindle checkpoint. Science 1995, 267:1353–1356
6. Fukasawa K, Choi T, Kuriyama R, Rulong S, van de Woude GF: Abnormal centrosome amplification in the absence of p53. Science 1996, 271:1744–1747
7. Rubio CA, Befrits R: Atypical mitoses in colectomy specimens from patients with long standing ulcerative colitis. Anticancer Res 1997, 17:2721–2726
8. Bystrevskaya VB, Lobova TV, Smirnov VN, Makarova NE, Kushch AA: Centrosome injury in cells infected with human cytomegalovirus. J Struct Biol 1997, 120:52–60
9. Pittman S, Geyp M, Fraser M, Ellem K, Peaston A, Ireland C: Multiple centrosomal microtubule organising centres and increased microtubule stability are early features of VP-16-induced apoptosis in CCRF-CEM cells. Leuk Res 1997, 21:491–499
10. Gualberto A, Aldape K, Kozakiewicz K, Tlsty TD: An oncogenic form of p53 confers a dominant, gain-of-function phenotype that disrupts spindle checkpoint control. Proc Natl Acad Sci USA 1998, 95:5166–5171
11. Cliby WA, Roberts CJ, Cimprich KA, Stringer CM, Lamb JR, Schreiber SL, Friend SH: Overexpression of a kinase-inactive ATR protein causes sensitivity to DNA-damaging agents and defects in cell cycle checkpoints. EMBO J 1998, 17:159–169
12. Hinchcliffe EH, Cassels GO, Rieder CL, Sluder G: The coordination of centrosome reproduction with nuclear events of the cell cycle in the sea urchin zygote. J Cell Biol 1998, 140:1417–1426
13. Yu YH, Xu FJ, Peng HQ, Fang XJ, Zhao SL, Li Y, Cuevas B, Kuo WL, Gray, JW, Siciliano M, Mills GB, Bast RC: NOEY2 (ARHI), an imprinted putative tumor suppressor gene in ovarian and breast carcinomas. Proc Natl Acad Sci USA 1999, 96:214–219
14. Lingle WL, Lutz WH, Ingle JN, Maihle NJ, Salisbury JL: Centrosome hypertrophy in human breast tumors: implications for genomic stability and cell polarity. Proc Natl Acad Sci USA 1998, 95:2950–2955
15. Pihan GA, Purohit A, Wallace J, Knecht H, Woda B, Quesenberry P, Doxsey SJ: Centrosome defects and genetic instability in malignant tumors. Cancer Res 1998, 58:3974–3985
16. Weber RG, Bridger JM, Benner A, Weisenberger D, Ehemann V, Reifenberger, Lichter P: Centrosome amplification as a possible mechanism for numerical chromosome aberrations in cerebral primitive neuroectodermal tumors with TP53 mutations. Cytogenet Cell Genet 1998, 83:266–269
17. Carroll PE, Okuda M, Horn HF, Biddinger P, Stambrook PJ, Gleich LL, Li YQ, Tarapore P, Fukasawa K: Centrosome hyperamplification in human cancer: chromosome instability induced by p53 mutation and/or Mdm2 overexpression. Oncogene 1999, 18:1935–1944
18. Zhou HY, Kuang J, Zhong L, Kuo WL, Gray JW, Sahin A, Brinkley BR: Tumour amplified kinase STK15/BTAK induces centrosome amplification, aneuploidy and transformation. Nat Genet 1998, 20:189–193
19. Kellogg DR, Moritz M, Alberts BM: The centrosome and cellular organization. Annu Rev Biochem 1994, 63:639–674
20. Rose MD, Biggins S, Satterwhite LL: Unravelling the tangled web at the microtubule-organizing center. Curr Opin Cell Biol 1993, 5:105–115
21. Chretien D, Buendia B, Fuller SD, Karsenti E: Reconstruction of the centrosome cycle from cryoelectron micrographs. J Struct Biol 1997, 120:117–133
22. Vorobjev IA, Chentsov YS: Centrioles in the cell cycle. I. Epithelial cells. J Cell Biol 1982 93:938–949
23. Alvey PL: An investigation of the centriole cycle using 3T3 and CHO cells. J Cell Sci 1985, 78:147–162

24. Robbins E, Jentzsch G, Micali A: The centriole cycle in synchronized HeLa cells. J Cell Biol 1968, 36:329–339
25. Compton DA: Focusing of spindle poles. J Cell Sci 1998, 111:1477–1481
26. Wheatley DN: Ultrastructure. I. The basic centriole. The Centriole: A Central Enigma of Biology. Amsterdam, Elsevier Biomedical Press, 1982, pp 21–49
27. Reinsch S, Karsenti E: Orientation of spindle axis and distribution of plasma membrane proteins during cell division in polarized MDCKII cells. J Cell Biol 1994, 126:1509–1526
28. Ferguson DJ: An ultrastructural study of mitosis and cytokinesis in normal 'resting' human breast. Cell Tissue Res 1988, 252:581–587
29. Olsson H, Jernstrom H, Alm P, Kreipe H, Ingvar C, Jonsson PE, Ryden S: Proliferation of the breast epithelium in relation to menstrual cycle phase, hormonal use, and reproductive factors. Breast Cancer Res Treat 1996, 40:187–196
30. Stirling JW, Chandler JA: Ultrastructural studies of the female breast. I. 9+0 cilia in myoepithelial cells. Anat Rec 1976, 186:413–416
31. Onishchenko GE: On the consistence between the number of centrioles and the ploidy in the hepatocytes in the mouse liver. Tsitologiia 1978, 20:395–399
32. Nagata Y, Muro Y, Todokoro K: Thrombopoietin-induced polyploidization of bone marrow megakaryocytes is due to a unique regulatory mechanism in late mitosis. J Cell Biol 1997, 139:449–457
33. Reilova-Velez J, Seiler MW: Abnormal cilia in a breast carcinoma. An ultrastructural study. Arch Pathol Lab Med 1984, 108:795–797
34. Sorokin SP: Reconstructions of centriole formation and ciliogenesis in mammalian lungs. J Cell Sci 1968, 3:207–230
35. Anderson RG, Brenner RM: The formation of basal bodies (centrioles) in the Rhesus monkey oviduct. J Cell Biol 1971, 50:10–34
36. Dirksen ER: Ciliary basal body morphogenesis: the early events. Symp Soc Exp Biol 1982, 35:439–463
37. Dirksen ER: Centriole and basal body formation during ciliogenesis revisited. Biol Cell 1991, 72:31–38
38. van den Steen P, van Lommel A, Lauweryns JM: Presence and possible implications of open-ring centrioles, multiple basal centrioles and basal cilia in neonatal hamster bronchioles. Acta Anat 1995, 153:85–95
39. McGill M, Highfield DP, Monahan TM, Brinkley BR: Effects of nucleic acid specific dyes on centrioles of mammalian cells. J Ultrastruct Res 1976, 57:43–53
40. Tournier F, Komesli S, Paintrand M, Job D, Bornens M: The intercentriolar linkage is critical for the ability of heterologous centrosomes to induce parthenogenesis in Xenopus. J Cell Biol 1991, 113:1361–1369
41. Lemullois M, Klotz C, Sandoz D: Immunocytochemical localization of myosin during ciliogenesis of quail oviduct. Eur J Cell Biol 1987, 43:429–437
42. Callaini G, Marchini D: Abnormal centrosomes in cold-treated Drosophila embryos. Exp Cell Res 1989, 184:367–374
43. Baron AT, Suman VJ, Nemeth E, Salisbury JL: The pericentriolar lattice of PtK2 cells exhibits temperature and calcium-modulated behavior. J Cell Sci 1994, 107:2993–3003
44. Moritz M, Zheng YX, Alberts BM, Oegema K: Recruitment of the γ-tubulin ring complex to Drosophila salt-stripped centrosome scaffolds. J Cell Biol 1998, 142:775–786

Centrosome amplification drives chromosomal instability in breast tumor development

Wilma L. Lingle*†‡§, Susan L. Barrett†, Vivian C. Negron*, Antonino B. D'Assoro†, Kelly Boeneman*, Wanguo Liu*, Clark M. Whitehead†, Carol Reynolds¶, and Jeffrey L. Salisbury†‡

*Division of Experimental Pathology, †Tumor Biology Program, and ¶Division of Anatomic Pathology, Mayo Clinic, Rochester, MN 55905

Edited by George F. Vande Woude, Van Andel Research Institute, Grand Rapids, MI, and approved December 12, 2001 (received for review September 11, 2001)

Earlier studies of invasive breast tumors have shown that 60–80% are aneuploid and ≈80% exhibit amplified centrosomes. In this study, we investigated the relationship of centrosome amplification with aneuploidy, chromosomal instability, p53 mutation, and loss of differentiation in human breast tumors. Twenty invasive breast tumors and seven normal breast tissues were analyzed by fluorescence *in situ* hybridization with centromeric probes to chromosomes 3, 7, and 17. We analyzed these tumors for both aneuploidy and unstable karyotypes as determined by chromosomal instability. The results were then tested for correlation with three measures of centrosome amplification: centrosome size, centrosome number, and centrosome microtubule nucleation capacity. Centrosome size and centrosome number both showed a positive, significant, linear correlation with aneuploidy and chromosomal instability. Microtubule nucleation capacity showed no such correlation, but did correlate significantly with loss of tissue differentiation. Centrosome amplification was detected in *in situ* ductal carcinomas, suggesting that centrosome amplification is an early event in these lesions. Centrosome amplification and chromosomal instability occurred independently of p53 mutation, whereas p53 mutation was associated with a significant increase in centrosome microtubule nucleation capacity. Together, these results demonstrate that independent aspects of centrosome amplification correlate with chromosomal instability and loss of tissue differentiation and may be involved in tumor development and progression. These results further suggest that aspects of centrosome amplification may have clinical diagnostic and/or prognostic value and that the centrosome may be a potential target for cancer therapy.

Mitotic fidelity and cytoplasmic organization are both consequences of normal centrosome function. Defective centrosomes, exemplified by an excess number of centrioles and pericentriolar material, are characteristic of breast tumors and solid tumors in general (reviewed in refs. 1–3). These observations have implicated the centrosome in the origin of chromosomal abnormalities in the development of malignant tumors (4–8). In this study, we investigate the relationship between centrosome amplification and aneuploidy, chromosomal instability (CIN), p53 mutation, and loss of tissue differentiation in human breast tumors.

Chromosomal abnormalities have long been recognized as a distinguishing feature of cancer cells (4). Fluorescence *in situ* hybridization (FISH) with centromeric probes is a sensitive technique that can detect aneusomy as numeric alterations of specific chromosomes (9–12). FISH and comparative genomic hybridization studies have shown that aneusomy may be an early event in breast tumor development (13, 14). FISH data from simultaneous detection of two or more chromosome probes can be analyzed to determine whether tissues are diploid or aneuploid, whether they are potentially polyploid, whether one or more clonal cell populations are present, and whether the chromosome number is stable (13, 14). CIN was first defined in colorectal cancers as the percent of cells with nonmodal chromosome number (15). CIN is a measure of the flux in karyotype, as opposed to aneuploidy, which describes the condition of a nondiploid karyotype. CIN is the *rate* of change in chromosome number, whereas aneuploidy is the *state* of an altered chromosome number (15).

In addition to alterations in chromosome number, most solid tumors are also characterized by centrosome amplification (1). Centrosomes nucleate and organize the cytoplasmic and mitotic spindle microtubules (MTs) in interphase and mitotic cells, respectively. It has been hypothesized that centrosome amplification affects cell and tissue architecture by altering the microtubule (MT) cytoskeleton (6, 16). Because the centrosome is actively involved in proper chromosome segregation during mitosis, it also has been hypothesized that centrosome amplification drives tumor aneuploidy by increasing the frequency of abnormal mitoses that lead to chromosome missegregation (4, 6, 16–18). Although earlier studies have suggested that centrosome amplification is a downstream consequence of p53 nullizygosity, or loss or gain of function mutations (19–21), alternative pathways not involving p53 mutation have also been demonstrated (16–18).

Three analytical measures useful in assessing centrosome amplification in tumors include centrosome size and centrosome number, which are structural measures, and centrosome MT nucleation capacity, which is a measure of function. Most often, structural centrosome amplification is measured by immunomicroscopy of cells or tissues by using antibodies against the centrosome proteins centrin, pericentrin, or γ-tubulin, followed by quantitative or subjective measurement of centrosome size and/or number (5–8). Two basic approaches to measure MT nucleation capacity have been used depending on whether cultured cells or frozen tissues are used: MT regrowth in living cultured cells or *in vitro* MT nucleation and growth in fresh frozen tissues (6, 7). In this study, we investigated the correlation of these three features of centrosome amplification with aneuploidy, CIN, p53 mutation, and loss of differentiation in breast tumors. We found that centrosome size and number both correlate with aneuploidy and CIN, and that centrosome MT nucleation capacity correlates with loss of differentiation. MT nucleation was significantly greater in tumors with p53 mutations. However, although the presence of p53 mutation correlated with aneuploidy, it did not correlate with CIN. Furthermore, we demonstrated that structural centrosome amplification is present in ductal carcinoma *in situ* (DCIS). Together, these results support the hypothesis (4, 6) that centrosome amplification is an early event in tumorigenesis that drives both chromo-

This paper was submitted directly (Track II) to the PNAS office.

Abbreviations: CIN, chromosomal instability; DCIS, ductal carcinoma *in situ*; FISH, fluorescence *in situ* hybridization; MT, microtubule.

‡These authors' laboratories contributed equally to this research.

§To whom reprint requests should be addressed. E-mail: lingle@mayo.edu.

The publication costs of this article were defrayed in part by page charge payment. This article must therefore be hereby marked "*advertisement*" in accordance with 18 U.S.C. §1734 solely to indicate this fact.

www.pnas.org/cgi/doi/10.1073/pnas.032479999

somal instability and loss of differentiation through independent centrosome functions.

Methods

Tissues. Human breast tissues were collected according to a protocol approved by the Mayo Clinic Internal Review Board. Portions of the tissues were snap-frozen in liquid nitrogen within 30 min of surgery and stored at −70°C until use. All tumors were graded according to the Nottingham grading system by a single pathologist (C.R.), using standard hematoxylin-and-eosin-stained sections from paraffin-embedded portions of the same tumor.

Centrosome Volume, Number, and Area. Centrosome volume and number were determined as described by using confocal microscopy for volume reconstruction of centrosomes immunolabeled with a monoclonal antibody against centrin (6). Determinations in this study were based on average values for all cells in four fields of view including a minimum of 50 cells. Alternatively, the centrosome area was determined by confocal microscopy and image analysis of immunofluorescence signal by using a polyclonal antibody against pericentrin (Covance, Berkeley, CA) Similar results were obtained with antibodies against the centrosomal protein γ-tubulin (data not shown; see refs. 6 and 22). On each tissue section, the average signal from five fibroblast centrosomes was used to normalize the values of epithelial cell centrosomes from five fields of view. Centrosome area was determined for 5 normal tissues from reduction mammoplasties, 7 DCIS tumors, 15 lymph node negative invasive ductal carcinomas, and 14 lymph node positive invasive ductal carcinomas. A normalized size and number index for centrosome amplification was calculated as follows: [(tumor centrosome size/0.023 μm^3) + (tumor centrosome number/1.55)]/2 = centrosome size and number index, where the average value for centrosome size in normal breast epithelial cells is 0.023 μm^3 and 1.55 is the average number of centrosomes in normal breast epithelial cells. Correlative light and electron microscopy on selected tissues demonstrated that multiple anti-centrin-staining spots corresponded to supernumerary centrioles and/or excess pericentriolar material (22).

MT Nucleation. The capacity of centrosomes to nucleate MTs was determined by using an *in vitro* assay on touch preparations from frozen tissues according to published methods (23). This functional assay reflects the *in vitro* ability of centrosomes to nucleate MTs under defined conditions where time, temperature, and tubulin concentration were maintained such that MT nucleation and growth occurred only in association with centrosomes and did not occur spontaneously. Normal and tumor preparations were assayed in parallel by using identical conditions. The number of MTs nucleated per cell was determined for 100 consecutively viewed cells. Cells with significant overlap of MT arrays were excluded from analysis, as were obviously damaged cells. A normalized MT index was calculated from these results by dividing the tumor MT number by 4.8 MT, the average number of MTs nucleated by normal breast epithelial cells.

FISH Analysis. FISH probes to pericentromeric regions of chromosomes 3 (CEP3), 7 (CEP7), and 17 (CEP17) (Vysis, Downers Grove, IL) were hybridized to touch preparations of nuclei from frozen tissues according to published methods (9, 10). Probes were labeled with SpectrumOrange (CEP3), SpectrumGreen (CEP7), and SpectrumAqua (CEP17) for simultaneous analysis. DNA was counterstained with 4′,6-diamidino-2-phenylindole before mounting coverslips. For each tissue, 100 consecutive nuclei were scored for the number of signals for each of the three probes per nucleus with methods described (10).

Classification of tissue ploidy was a two-step process. In the first step, each of the 100 cells for a given tissue was classed as disomic if all three probes had two signals, as polysomic if two or more probes had more than two signals, as monosomic for a given probe, or otherwise as nondisomic. For the second step, the sum of the cells in each of the categories above was used to determine the tissue status as follows: (*i*) diploid if at least 50% of the cells were disomic, fewer than 15% were polysomic, and fewer than 50% were monosomic for the same chromosome, (*ii*) monosomic if 75% of the cells had the same chromosome loss and fewer than 15% were polysomic, or (*iii*) aneuploid if more than 15% of the cells were polysomic. Results from the seven reduction mammoplasties (assumed to be diploid) were used to calculate these cutoff values.

Cell clones were identified by evaluating the percentage of cells having identical probe signal patterns (24). A cell population with the same probe signal pattern was considered clonal if it represented at least 10% of the total cells. In tissues with high clonal heterogeneity, fewer than 10% of the cells had identical probe signal patterns. Tissues were considered to have low clonal heterogeneity if more than 20% of the cells were clonal, and one or two clones, each accounting for at least 10% of the total cells, could be identified.

The modal signal number of each chromosome was determined for each tissue. Bimodal values emerged in six tissues that had clones representing a significant percentage of the population. As described (15, 17), CIN was calculated for each chromosome as the percent of cells with nonmodal signal numbers. However, in this study, bimodal values were included in the calculation to minimize artificial inflation of CIN values. The average CIN values for the seven normal tissues plus and minus three standard deviations was used to identify tumors with unstable karyotypes.

p53 Mutation Analysis. Denaturing high-performance liquid chromatography was used to screen tissues for p53 mutations according to published methods (25). DNA was extracted from frozen sections of 7 reduction mammoplasties and 20 invasive tumors (the same tissues that were analyzed by FISH). Six regions of genomic DNA, which included exons 4–9 and spanned the splice sites, were amplified in separate PCRs. Amplified DNA was separated under partial denaturing conditions by using a WAVE System denaturing high-performance liquid chromatography (Transgenomic, San Jose, CA), and the resulting curves were compared with curves for wild-type p53. DNA from curves that did not conform to the wild-type profile was sequenced to confirm and identify mutations.

Statistical Analysis. Linear regression analysis with Kendall's τ test was used to determine that CIN for chromosomes 3, 7, and 17 each correlate with centrosome size and number ($P < 0.05$), but not with MT nucleation capacity. Significance of differences in centrosome size, number, and MT nucleation capacity between ploidy groups, and in MT nucleation capacity between the different grades of tumor, and in MT nucleation capacity between tumors with wild-type or mutant p53 was determined by using the Wilcox rank-sum test.

Results

FISH Analysis. FISH data were analyzed to establish ploidy and to identify tumors with unstable karyotypes. Three of 20 invasive tumors were diploid, with chromosome gains and losses falling well within the range of normal values (Figs. 1 and 2 *A* and *B*). Three additional tumors were classified as monosomic for chromosome 17, because more than 75% of the cells had only one chromosome 17 signal with no other significant chromosome aberrations (Fig. 2*B*). None of the tumors were monosomic for chromosomes 3 or 7 (Fig. 2*B*). Fourteen of the 20 invasive tumors were aneuploid. This group of aneuploid tumors was

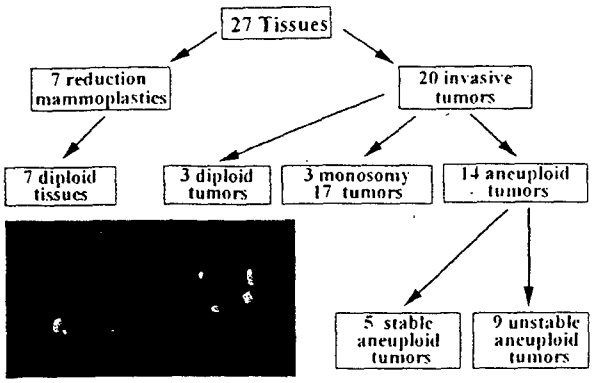

Fig. 1. FISH analysis. Flow chart of human breast tissue and tumor classification used in this study based on FISH analysis for chromosomes 3, 7, and 17. (*Inset*) FISH signals from two representative tumor nuclei: red signal, chromosome 3; green signal, chromosome 7; blue signal, chromosome 17.

subdivided into a group of 5 tumors with normal CIN values and another group of 9 tumors with high CIN values (Figs. 1 and 2 *A* and *B* and Table 1, which is published as supporting information on the PNAS web site, www.pnas.org). The five aneuploid tissues with near-normal CIN values are examples of tumors with stable, but aneuploid, karyotypes. The nine tumors with high CIN are examples of tumors with karyotypes in a state of flux.

Centrosome Amplification. In Fig. 2*B*, centrosome amplification (*Lower*) and chromosome gains and losses (*Upper*) for each individual tissue are shown. A clear positive association was apparent between increasing centrosome amplification and chromosomal gains and losses (Fig. 2*B*). Centrosome volume and centrosome number in normal tissues averaged 0.023 μm^3 and 1.55, respectively (Table 1, Figs. 2 *B* and *C* and 3*A*). Two centrosome amplification indices for each tissue are presented in Fig. 2*B Lower*: the size and number index (yellow bars) reflects the combined normalized contributions of centrosome size and centrosome number, and the MT nucleation index (maroon bars) reflects the normalized MT nucleation capacity. Average centrosome volume of the stable aneuploid tumors was 0.112 μm^3 and average volume of unstable aneuploid tumors was 0.198 μm^3, more than 5- and 8-fold greater than normal values (0.023 μm^3), respectively (Fig. 2*C Upper*). Immunofluorescence of centrosome size and number for each of the ploidy groups are presented in Fig. 3 *A–E*. Centrosome volume in the 14 aneuploid tumors spanned a wide range, indicating a high degree of variability among tumors. Monosomy 17 and diploid tumors had

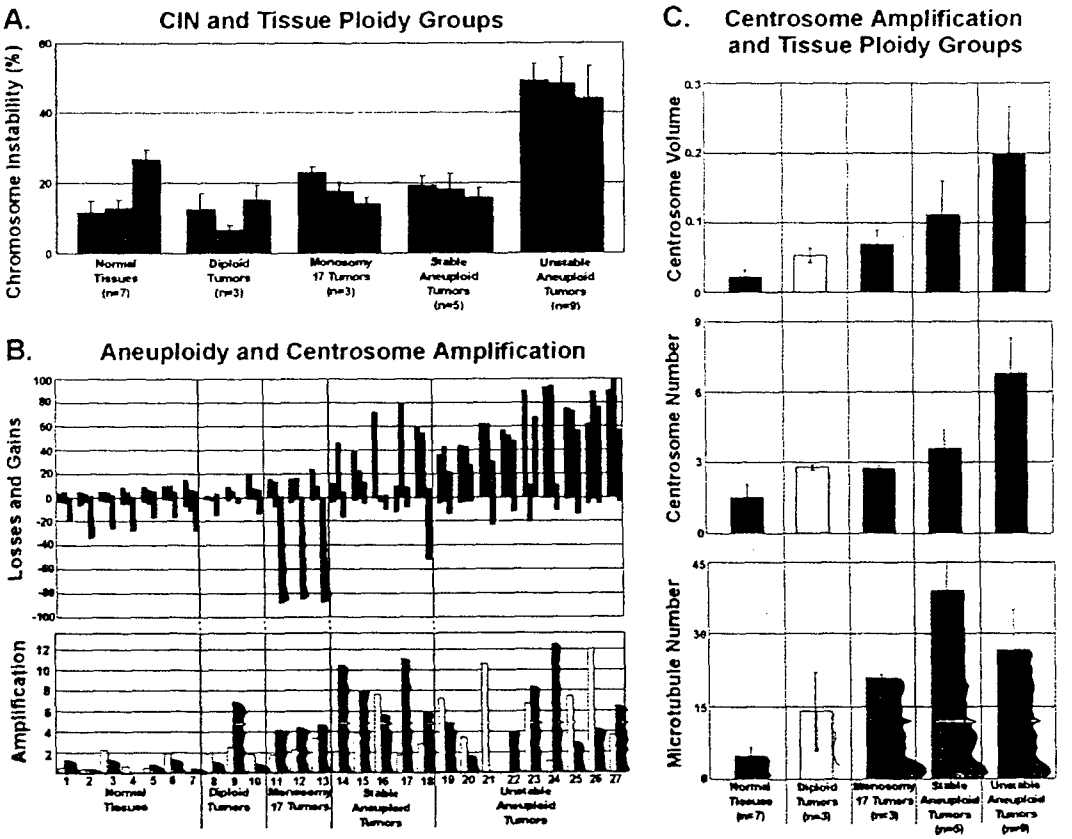

Fig. 2. Analysis of chromosomal instability, aneuploidy, and centrosome amplification for the five tissue ploidy groups. (*A*) Plot of CIN (% cells showing chromosome number differing from the modal value for that particular chromosome) for the various tissue ploidy groups. (*B*) Plots of aneuploidy and centrosome amplification. (*Upper*) Plot of chromosome losses and gains for each sample in each tissue ploidy group. For both *A* and *B*: red bars, chromosome 3; green bars, chromosome 7; blue bars, chromosome 17. (*Lower*) Plot of centrosome amplification for each sample in each tissue ploidy group. Yellow bars, normalized centrosome size and number index; maroon bars, normalized microtubule nucleation index. (*C*) Plots of three different measures of centrosome amplification (centrosome volume in μm^3, centrosome number, and microtubule nucleation) for each tissue ploidy group. Bars in *A* and *C* indicate standard deviation.

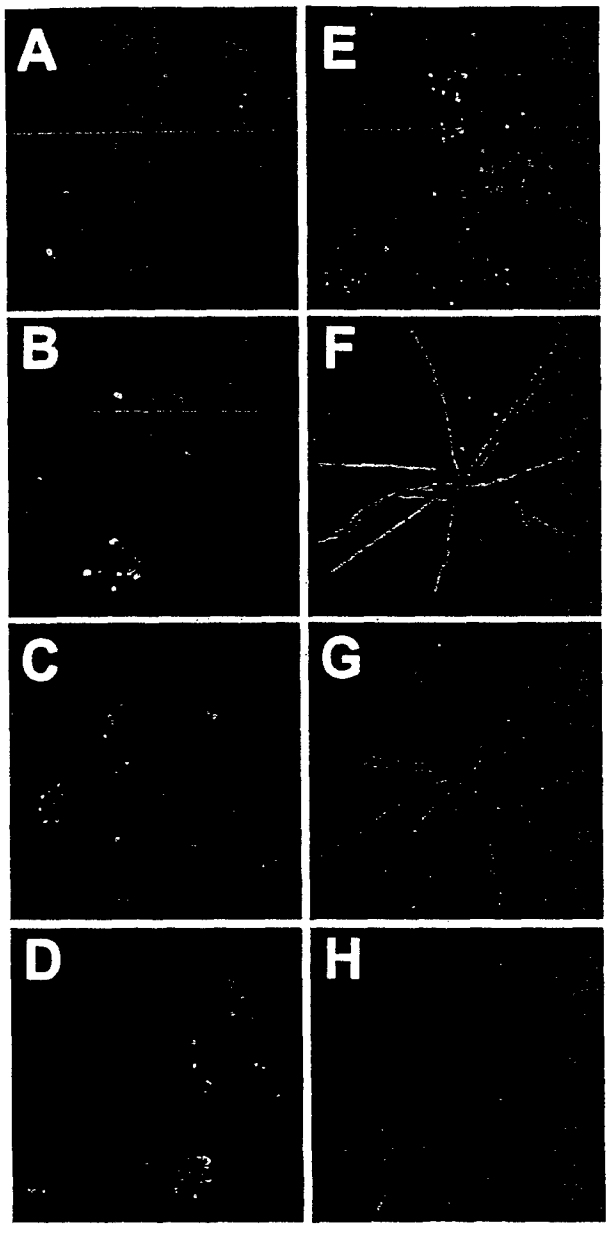

Fig. 3. Examples of immunofluorescence of centrosomes stained for centrin (green) in normal breast tissue (*A*) and centrosome amplification in breast tumors (*B–E*) and for microtubule nucleation (*F–H*) (green, anti-tubulin). (*A*) Region of a normal breast duct (lumen, center right) showing nuclei (red) located in the basal region of epithelial cells and pairs of centrioles (green, anti-centrin) located apically. (*B–E*) Examples of breast tumors showing the range of centrosome amplification in tumor tissue: (*B*) Diploid tumor. (*C*) Monosomy 17 tumor. (*D*) Stable aneuploid tumor. (*E*) Unstable aneuploid tumor. (*F–H*) Three examples of microtubule nucleation in touch preparations of breast tumor cells: (*F*) Diploid tumor. (*G*) Monosomy 17 tumor. (*H*) Stable aneuploid tumor.

centrosome volumes intermediate between normal and aneuploid tumors (Figs. 2*C Top* and 3 *A–C*).

Centrosome number was significantly greater in the unstable aneuploid tumors than in normal tissues ($P < 0.02$) (Figs. 2*C Middle* and 3 *A–E*). Unstable aneuploid tumors had an average centrosome number of 6.8 centrosomes per cell compared with 3.6 (stable aneuploid tumors), 2.7 (monosomy 17 tumors), 2.8 (diploid tumors), and 1.5 (normal tissues). Centrosome numbers in diploid and monosomy 17 tumors were not significantly different from each other, but were nearly 2-fold greater than in normal tissues.

Centrosomes of two of the three diploid tumors had MT nucleation capacity indistinguishable from normal tissues, whereas one diploid tumor nucleated significantly more MTs (Fig. 2*B Lower*). All other tumors had a higher MT nucleation capacity than did normal tissues (Figs. 2*B Bottom* and 3 *F* and *G*). Normal tissues showed significantly lower MT nucleation than monosomy 17 tumors ($P < 0.02$), stable aneuploid tumors ($P < 0.005$), and unstable aneuploid tumors ($P < 0.01$). On average, however, MT nucleation capacity was not significantly different between diploid tumors, monosomy 17 tumors, and unstable aneuploid tumors (Fig. 2*C Bottom*). Only stable aneuploid tumors had a MT nucleation capacity significantly higher than monosomy 17 tumors ($P < 0.04$) (Fig. 2*C Bottom*). Although stable aneuploid tumors nucleated more MTs than unstable aneuploid tumors, the difference was not statistically significant (Fig. 2*C Bottom*).

Centrosome Amplification in Preinvasive and Invasive Lesions. Centrosomes in normal breast epithelial tissues showed a consistent and narrow range of size with a standard deviation less than 7% of the average value, indicated by the horizontal bar in Fig. 4*A*. The centrosomes in noninvasive DCIS tumors displayed significant amplification in size, similar in range to that of both lymph negative and lymph node positive invasive tumors (Fig. 4*A*). FISH was not performed on these tissues.

p53 Mutation Analysis. The seven normal tissues from reduction mammoplasties had wild-type p53 (Table 1). Of 20 invasive tumors, we identified 5 with mutant p53. These mutations were all in the DNA-binding domain. All 5 tumors with p53 mutations were aneuploid, 2 had stable karyotypes (low CIN), and 3 had unstable karyotypes (high CIN). None of the diploid or monosomy 17 tumors had p53 mutations. Only tumors with sequence-confirmed p53 mutation were positive for p53 by immunohistochemistry, and only those positive by immunohistochemistry had sequence-confirmed mutations (data not shown).

Statistical Correlations. When plotted against the CIN values for each of the three chromosomes, both centrosome number and centrosome volume of individual tumors showed significant, positive, linear correlations ($P < 0.04$) (Fig. 4 *B* and *C*). MT nucleation capacity did not correlate with CIN values for any of the three chromosomes (Fig. 4*D*). However, MT nucleation capacity did correlate with loss of tissue differentiation for Nottingham grades 2 and 3 compared with normal tissue ($P < 0.01$) as illustrated in Fig. 4*E*. Average MT nucleation was significantly greater in p53 mutant tumors than in all other tissue groups, including aneuploid p53 wild-type tumors, nondiploid p53 wild-type tumors, and normal tissues (Fig. 4*A*, Table 1).

Discussion

Studies in cell lines have implicated centrosome defects in abnormal mitoses leading to genomic instability in breast (17), pancreas (8), colon (26), and prostate (16) cancers. Here we demonstrate by using primary breast tumors that two aspects of centrosome amplification correlate independently with distinct features of breast cancer. Increased centrosome size and centrosome number correlate with CIN. We demonstrated that increased centrosome size is present in most *in situ* lesions, supporting the hypothesis that centrosome abnormalities drive chromosomal aberrations as an early event in DCIS. In addition, increased MT nucleation capacity of centrosomes correlated with loss of tissue differentiation. Loss of differentiation as

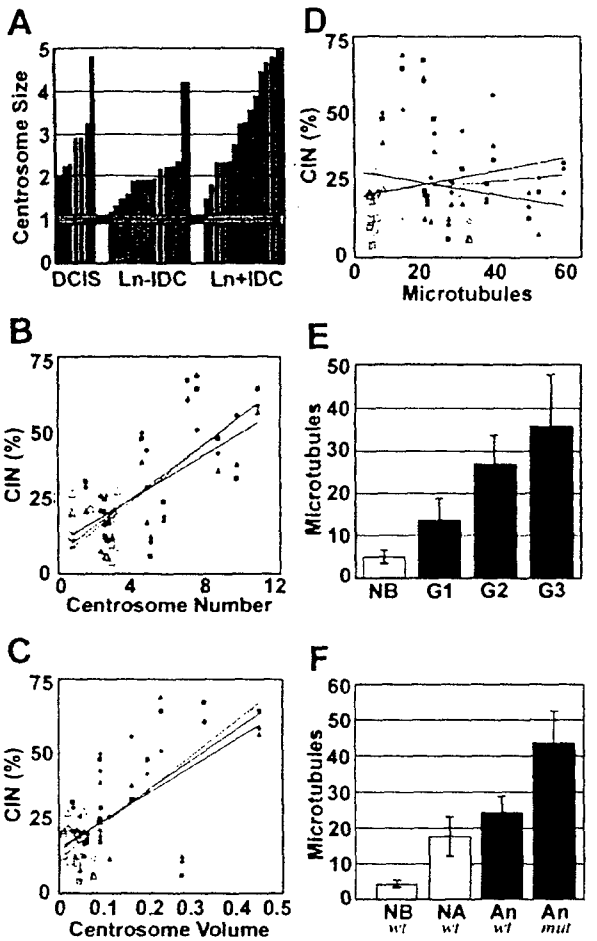

Fig. 4. (*A*) Analysis of centrosome amplification, CIN, Nottingham grade, and p53 mutations. Bar graph of centrosome amplification normalized against fibroblast centrosomes for individual DCIS, lymph node negative invasive ductal carcinoma (Ln-IDC), and lymph node positive invasive ductal carcinoma (Ln+IDC). Gray horizontal bar indicates average for five normal breast epithelial tissues including standard error. (*B–D*) Plots of CIN and centrosome amplification. CIN (%) for each tissue and each chromosome is plotted against centrosome number (*B*), centrosome volume (μm^3) (*C*), and microtubule nucleation (*D*). Open symbols are values for normal breast tissue, gray-filled symbols are values for diploid tumors, and closed symbols are values for aneuploid tumor tissue. Red symbols, chromosome 3; green symbols, chromosome 7; blue symbols, chromosome 17. (*E*) Bar graph of microtubule nucleation for normal breast tissue (NB) and tumors of Nottingham grades G1, G2, and G3. (*F*) Bar graph of microtubule nucleation and p53 status (wild type, *wt*; mutant, *mut*) for normal breast tissue (NB), nonaneuploid (diploid + monosomy 17) tumors (NA), and aneuploid tumors (An). Bars in *E* and *F* indicate standard deviation.

indicated by high histologic grade is an indicator of poor prognosis (27), probably because of the increased metastatic potential of cells with altered cytoskeletons and adherent properties (28).

We also demonstrated that centrosome amplification and aneuploidy occur independently of p53 mutation. Of 14 aneuploid tumors, all of which had structurally amplified centrosomes, 9 had wild-type p53 and 5 had mutant p53. The frequency of CIN was the same in aneuploid tumors with wild-type (6 of 10) or mutant p53 (3 of 5), therefore mutant p53 did not correlate with CIN in aneuploid tumors, indicating that although aneuploidy can arise in the absence of p53 mutation, aneuploidy occurred only in the presence of centrosome amplification, in the tissues studied here, regardless of p53 mutation status. Therefore, molecular alterations other than p53 mutation may induce centrosome amplification with the potential to drive CIN.

The frequencies of aneusomy presented here are similar to published FISH data in breast tissues (10, 14). Studies have shown that the use of probes for just two chromosomes was sufficient to segregate diploid from aneuploid tumors (29, 30). However, an advantage to the use of more than two probes is that clonal populations can be identified with greater certainty (24). High clonal heterogeneity is the likely result of aneuploidy originating directly through chromosomal instability generating multiple unrelated clones, rather than through a linear model in which endoreduplication is followed by gains and losses of chromosomes (24, 31). Here, the simultaneous use of three probes allowed us to identify six tumors that contained two clones, each of which comprised greater than 25% of the tumor cell population. We adjusted the CIN values of these tumors with low clonal heterogeneity to reflect bimodal chromosome values, thus avoiding artificial inflation of CIN values and enabling us to identify accurately five aneuploid tumors with low clonal heterogeneity and stable karyotypes (i.e., low CIN) separately from nine aneuploid tumors with high clonal heterogeneity and unstable karyotypes (high CIN). These two groups of tumors are significantly different from each other with regard to their centrosome characteristics. The unstable aneuploid tumors (high CIN) had significantly larger centrosomes and more numerous centrosomes than did the stable aneuploid tumors (low CIN). The stable aneuploid tumors described here may have regained normal centrosome function by coalescence of supernumerary centrosomes (1, 22) and thereby acquired a growth advantage, because their normal bipolar mitotic spindles faithfully segregate the successful aneuploid karyotype. That the aneuploidy found in these stable aneuploid tumors originated through centrosome amplification, and not some other mechanism, is evidenced by their retention of increased MT nucleation capacity as an independent aspect of centrosome amplification. Likewise, in an experimental cell culture system, Chiba and coworkers (32) found that chromosomal instability and centrosome amplification underwent a "convergence" to stable aneuploidy and normal centrosome numbers with continued passage in culture. Therefore, we suggest that the stable aneuploid tumors identified here may have evolved through convergence in tumors originally having high clonal heterogeneity, and that both groups of aneuploid tumors were initiated by chromosomal instability caused by amplified centrosomes.

Our results demonstrate that increased MT nucleation capacity is a feature of centrosome amplification that is independent of centrosome number and centrosome size in breast tumors. Although MT nucleation capacity did not correlate with CIN or aneuploidy, it was significantly greater in p53 mutant aneuploid tumors than in those with wild-type p53. MT nucleation capacity did correlate with increased Nottingham grade, suggesting a relationship between defects in the MT cytoskeleton and loss of tissue differentiation. In single- and multicenter studies, Nottingham grade predicted clinical outcome, with increasing grade being associated with shorter disease-free survival and overall survival (33, 34). Likewise, centrosome amplification correlates with loss of differentiation as defined by increased Gleason score in prostate tumors (16). Together these observations implicate alterations in functional properties of centrosomes in maintaining the morphological changes associated with tumor development.

Although p53 mutation has been implicated as a cause for CIN in breast cancer (35), our results, and results from other studies (36, 37), demonstrate that aneuploidy and CIN occur more often in the absence of p53 mutation. However, they do not occur in

the absence of structural centrosome amplification. Although mutant p53 is present in a significant portion of breast tumors, its occurrence is not a prerequisite to the development of aneuploidy. In the cases where mutant p53 is a factor, it is likely that p53 mutation affects centrosome number to promote abnormal mitoses (5, 20, 32). Our studies further demonstrate that p53 mutations correlate with a significant increase in the MT nucleation capacity of centrosomes.

In summary, our studies demonstrate that centrosome amplification is an early event in the development of breast cancer, and amplification of centrosome size and number correlate with CIN. Furthermore, centrosome amplification and CIN occur independently of p53 mutation in aneuploid tumors. Finally, MT nucleation capacity is an independent feature of centrosome amplification that correlates with loss of differentiation and is also increased significantly in tumors with p53 mutations. Because centrosome amplification precedes nuclear changes associated with aneuploidy in experimental systems (38) and is present in breast DCIS, it is possible that centrosome amplification drives CIN in breast tumor development. We suggest that centrosome amplification may increase metastatic potential through cytoskeletal alterations that affect tissue architecture in breast tumors. Although p53 mutations may exacerbate centrosome amplification, in this study they were not associated with an increased frequency of CIN. Centrosome amplification may be an indicator of CIN and unstable karyotypes in breast cancer that could be used to identify a subset of patients who would benefit from initial aggressive treatment. Finally, the centrosome presents a potential target for therapies against breast cancer through regulation of centrosome duplication and separation and through suppression of MT nucleation function.

We thank Drs. R. B. Jenkins, S. N. Thibodeau, N. J. Maihle, D. J. O'Kane, and D. Farrugia for critical review of the manuscript, Dr. S. J. Iturria for statistical analyses, and Mr. J. Tarara of the Mayo Optical Morphology Core Facility for his advice and technical assistance. This work was supported by DAMD 17-98-1-8122 from the Department of Defense Breast Cancer Research Program (to W.L.L.), by Grant CA72836 from the National Cancer Institute (to J.L.S.), and by the Mayo Foundation.

1. Brinkley, B. R. (2001) *Trends Cell Biol.* **11**, 18–21.
2. Lingle, W. L. & Salisbury, J. L. (2000) *Curr. Top. Dev. Biol.* **49**, 313–329.
3. Salisbury, J. L. (2001) *J. Mammary Gland Biol. Neoplasia* **6**, 203–212.
4. Boveri, T. (1914) *Zur Frage der Entstehung Maligner Tumoren* (Fischer, Jena); trans. Boveri, M. (1929) *The Origin of Malignant Tumors* (Williams and Wilkins, Baltimore) (English).
5. Carroll, P. E., Okuda, M., Horn, H. F., Biddinger, P., Stambrook, P. J., Gleich, L. L., Li, Y. Q., Tarapore, P. & Fukasawa, K. (1999) *Oncogene* **18**, 1935–1944.
6. Lingle, W. L., Lutz, W. H., Ingle, J. N., Maihle, N. J. & Salisbury, J. L. (1998) *Proc. Natl. Acad. Sci. USA* **95**, 2950–2955.
7. Pihan, G. A., Purohit, A., Wallace, J., Knecht, H., Woda, B., Quesenberry, P. & Doxsey, S. J. (1998) *Cancer Res.* **58**, 3974–3985.
8. Sato, N., Mizumoto, K., Nakamura, M., Machara, N., Minamishima, Y. A., Nishio, S., Nagai, E. & Tanaka, M. (2001) *Cancer Genet. Cytogenet.* **126**, 13–19.
9. Halling, K. C., King, W., Sokolova, I. A., Meyer, R. G., Burkhardt, H. M., Halling, A. C., Cheville, J. C., Sebo, T. J., Ramakumar, S., Stewart, C. S., *et al.* (2000) *J. Urol.* **164**, 1768–1775.
10. Persons, D. L., Robinson, R. A., Hsu, P. H., Seelig, S. A., Borell, T. J., Hartmann, L. C. & Jenkins, R. B. (1996) *Clin. Cancer Res.* **2**, 883–888.
11. Pinkel, D., Straume, T. & Gray, J. W. (1986) *Proc. Natl. Acad. Sci. USA* **83**, 2934–2938.
12. Rennstam, K., Baldetorp, B., Kytola, S., Tanner, M. & Isola, J. (2001) *Cancer Res.* **61**, 1214–1219.
13. Mendelin, J., Grayson, M., Wallis, T. & Visscher, D. W. (1999) *Lab. Invest.* **79**, 387–393.
14. Tirkkonen, M., Tanner, M., Karhu, R., Kallioniemi, A., Isola, J. & Kallioniemi, O. P. (1998) *Genes Chromosomes Cancer* **21**, 177–184.
15. Lengauer, C., Kinzler, K. & Vogelstein, B. (1997) *Nature (London)* **386**, 623–627.
16. Pihan, G. A., Purohit, A., Wallace, J., Malhotra, R., Liotta, L. & Doxsey, S. J. (2001) *Cancer Res.* **61**, 2212–2219.
17. Miyoshi, Y., Iwao, K., Egawa, C. & Noguchi, S. (2001) *Int. J. Cancer* **92**, 370–373.
18. Zhou, H., Kuang, J., Zhong, L., Kuo, W. L., Gray, J. W., Sahin, A., Brinkley, B. R. & Sen, S. (1998) *Nat. Genet.* **20**, 189–193.
19. Wang, X. J., Greenhalgh, D. A., Jiang, A., He, D., Zhong, L., Medina, D., Brinkley, B. R. & Roop, D. R. (1998) *Oncogene* **17**, 35–45.
20. Fukasawa, K., Choi, T., Kuriyama, R., Rulong, S. & Vande Woude, G. F. (1996) *Science* **271**, 1744–1747.
21. Weber, R. G., Bridger, J. M., Benner, A., Weisenberger, D., Ehemann, V., Reifenberger, G. & Lichter, P. (1998) *Cytogenet. Cell Genet.* **83**, 266–269.
22. Lingle, W. L. & Salisbury, J. L. (1999) *Am. J. Pathol.* **155**, 1941–1951.
23. Lingle, W. L. & Salisbury, J. L. (2001) *Methods Cell Biol.* **67**, 325–336.
24. Farabegoli, F., Santini, D., Ceccarelli, C., Taffurelli, M., Marrano, D. & Baldini, N. (2001) *Cytometry* **46**, 50–56.
25. Liu, W., Smith, D. I., Rechtzigel, K. J., Thibodeau, S. N. & James, C. D. (1998) *Nucleic Acids Res.* **26**, 1396–1400.
26. Ghadimi, B. M., Sackett, D. L., Difilippantonio, M. J., Schrock, E., Neumann, T., Jauho, A., Auer, G. & Ried, T. (2000) *Genes Chromosomes Cancer* **27**, 183–190.
27. Fitzgibbons, P. L., Page, D. L., Weaver, D., Thor, A. D., Allred, D. C., Clark, G. M., Ruby, S. G., O'Malley, F., Simpson, J. F., Connolly, J. L., *et al.* (2000) *Arch. Pathol. Lab. Med.* **124**, 966–978.
28. Engers, R. & Gabbert, H. E. (2000) *J. Cancer Res. Clin. Oncol.* **126**, 682–692.
29. Fiegl, M., Kaufmann, H., Zojer, N., Schuster, R., Wiener, H., Mullauer, L., Roka, S., Huber, H. & Drach, J. (2000) *Hum. Pathol.* **31**, 448–455.
30. Takami, S., Kawasome, C., Kinoshita, M., Koyama, H. & Noguchi, S. (2001) *Clin. Chim. Acta* **308**, 127–131.
31. Kuukasjarvi, T., Karhu, R., Tanner, M., Kahkonen, M., Schaffer, A., Nupponen, N., Pennanen, S., Kallioniemi, A., Kallioniemi, O. P. & Isola, J. (1997) *Cancer Res.* **57**, 1597–1604.
32. Chiba, S., Okuda, M., Mussman, J. G. & Fukasawa, K. (2000) *Exp. Cell Res.* **258**, 310–321.
33. Elston, C. W. & Ellis, I. O. (1991) *Histopathology* **19**, 403–410.
34. Page, D. L., Gray, R., Allred, D. C., Dressler, L. G., Hatfield, A. K., Martino, S., Robert, N. J. & Wood, W. C. (2001) *Am. J. Clin. Oncol.* **24**, 10–18.
35. Sigurdsson, S., Bodvarsdottir, S. K., Anamthawat-Jonsson, K., Steinarsdottir, M., Jonasson, J. G., Ogmundsdottir, H. M. & Eyfjord, J. E. (2000) *Cancer Genet. Cytogenet.* **121**, 150–155.
36. Lavarino, C., Corletto, V., Mezzelani, A., Della Torre, G., Bartoli, C., Riva, C., Pierotti, M. A., Rilke, F. & Pilotti, S. (1998) *Br. J. Cancer* **77**, 125–130.
37. Sauer, T., Beraki, K., Jebsen, P. W., Ormerod, E. & Naess, O. (1998) *APMIS* **106**, 921–927.
38. Duensing, S., Duensing, A., Crum, C. P. & Munger, K. (2001) *Cancer Res.* **61**, 2356–2360.

DEPARTMENT OF THE ARMY
US ARMY MEDICAL RESEARCH AND MATERIEL COMMAND
504 SCOTT STREET
FORT DETRICK, MD 21702-5012

REPLY TO
ATTENTION OF

MCMR-RMI-S (70-1y) 15 May 03

MEMORANDUM FOR Administrator, Defense Technical Information Center (DTIC-OCA), 8725 John J. Kingman Road, Fort Belvoir, VA 22060-6218

SUBJECT: Request Change in Distribution Statement

1. The U.S. Army Medical Research and Materiel Command has reexamined the need for the limitation assigned to technical reports written for this Command. Request the limited distribution statement for the enclosed accession numbers be changed to "Approved for public release; distribution unlimited." These reports should be released to the National Technical Information Service.

2. Point of contact for this request is Ms. Kristin Morrow at DSN 343-7327 or by e-mail at Kristin.Morrow@det.amedd.army.mil.

FOR THE COMMANDER:

Encl

PHYLIS M. RINEHART
Deputy Chief of Staff for
Information Management

ADB266022
ADB260153
ADB272842
ADB283918
ADB282576
ADB282300
ADB285053
ADB262444
ADB282296
ADB258969
ADB269117
ADB283887
ADB263560
ADB262487
ADB277417
ADB285857
ADB270847
ADB283780
ADB262079
ADB279651
ADB253401
ADB264625
ADB279639
ADB263763
ADB283958
ADB262379
ADB283894
ADB283063
ADB261795
ADB263454
ADB281633
ADB283877
ADB284034
ADB283924
ADB284320
ADB284135
ADB259954
ADB258194
ADB266157
ADB279641
ADB244802
ADB257340
ADB244688
ADB283789
ADB258856
ADB270749
ADB258933
ADB265793
ADB281613
ADB284934
ADB263442
ADB284977
ADB263437
ADB265310
ADB281573
ADB250216
ADB258699
ADB274387
ADB285530